UNIVERSITY OF TURKU

OLD ACQUAINTANCES AND NEW PERSPECTIVES INTO TESTICULAR DEVELOPMENT AND FUNCTION

Sheyla Cisneros Montalvo

UNIVERSITY OF TURKU

OLD ACQUAINTANCES AND NEW PERSPECTIVES INTO TESTICULAR DEVELOPMENT AND FUNCTION

Sheyla Cisneros Montalvo

University of Turku

Faculty of Medicine
Institute of Biomedicine
Physiology
Turku Doctoral Programme of Molecular Medicine (TuDMM)

Supervised by

Professor Jorma Toppari, MD, PhD
Research Centre for Interactive
Physiology and Pharmacology
Institute of Biomedicine and Centre for
Population Health Research
University of Turku
Department of Pediatrics
Turku University Hospital
Turku, Finland

Mirja Nurmio, Ph.D.
Research Centre for Interactive
Physiology and Pharmacology
Institute of Biomedicine and Centre for
Population Health Research
University of Turku
Department of Pediatrics
Turku University Hospital
Turku, Finland

Reviewed by

Anne Jørgensen, Ph.D.
Dept. of Growth and Reproduction
Righospitalet
Copenhagen, Denmark

Docent Timo Tuuri, Ph.D.
Department of Obstetrics and Gynecology
Helsinki University Hospital
Helsinki, Finland

Opponent

Associate Professor Serge Nef, Ph.D.
Department of Genetic Medicine and
Development
University of Geneva
Geneva, Switzerland

To my lovely and encouraging family

UNIVERSITY OF TURKU
Faculty of Medicine
Institute of Biomedicine
Physiology
Turku Doctoral Programme of Molecular Medicine (TuDMM)
SHEYLA CISNEROS MONTALVO: Old acquaintances and new
perspectives into testicular development and function
Doctoral Dissertation, 191 pp.
November 2020

ABSTRACT

Testicular development and function are complex processes that involve synchronization of the proliferation, apoptosis, and differentiation of specific somatic and germ cells to ensure lifelong fertility. Dysregulation of the signaling pathways or molecular mechanisms underlying these biological events often causes male infertility. With the increase observed in male fertility disorders worldwide, it is important to understand the origin of these conditions to be able to develop therapeutic strategies to alleviate or cure them in the future. The aim of this thesis is to describe the function of specific proteins in testicular development and function.

Upstream stimulatory factor 1 (USF1) is a transcription factor that plays multiple roles in biological systems. In the testis, USF1 is reported to be expressed in Sertoli cells (SCs) and to bind specific genes during the differentiation of SCs. However, it remains elusive whether USF1 plays a role during spermatogenesis. Retinoblastoma protein (RB) and its associated E2F3 transcription factor are the regulators of various cellular events, such as mitosis, apoptosis, meiosis, and differentiation. We have previously shown that RB and E2F3 regulate adult SC function in the testis; however, the mechanism underlying this regulatory process is still unclear. Plasmalemma vesicle-associated protein is an endothelial-cell-specific membrane protein that is expressed in stomatal and fenestral diaphragms of a subset of endothelial cells. This protein regulates vascular permeability, leukocyte migration, and angiogenesis in different tissues; however, its role in the function of the testis has not yet been elucidated.

Overall, this thesis comprises four studies. In the first study, a flow-cytometry-based method is developed to allow the rapid cell composition screening of fresh and cultured testicular tissues. In the second study, USF1 was shown to be expressed in spermatogonial stem cells, where it regulates the balance between spermatogonial stem cell self-renewal and differentiation. In the third study, the role of E2F3 during testicular development and the interaction between E2F3 and RB to maintain adult SC function were investigated. In the last study, the importance of plasmalemma vesicle-associated protein is revealed in the endocrine regulation of the testis.

KEYWORDS: flow cytometry, USF1, spermatogonial stem cell, RB, E2F3, Sertoli cell, PLVAP

TIIVISTELMÄ

Kiveksen kehitys ja siittiötuotanto ovat monimutkaisia ja tarkoin säädeltyjä prosesseja. Somaattisten solujen ja itusolujen oikea-aikainen jakautuminen, solukuolema ja erilaistuminen ovat edellytyksenä miesten elinikäiselle hedelmällisyydelle. Miesten hedelmällisyyden häiriöt ovat lisääntyneet maailmanlaajuisesti, minkä vuoksi on tärkeää ymmärtää niiden syntyyn vaikuttavia molekulaarisia ja solutason mekanismeja, jotta tulevaisuudessa voidaan kehittää hoitoja niiden lievittämiseksi ja parantamiseksi.

'Upstream stimulatory factor 1 (USF1)' on transkriptiotekijä, jolla on useita tehtäviä eri kudoksissa. Kiveksessä sitä tiedetään tuotettavan Sertolin soluissa, joissa se niiden erilaistuessa sitoutuu useiden geenien säätelyalueille. On kuitenkin epäselvää, mikä on USF1:n merkitys hiiren siittiötuotannossa. Retinoblastoomaproteiini (RB) ja siihen liittyvä transkriptiotekijä E2F3 säätelevät useita solun tapahtumia, kuten jakautumista, solukuolemaa, meioosia ja erilaistumista. Olemme aiemmin osoittaneet, että kiveksessä RB yhdessä E2F3:n kanssa säätelee Sertolin solujen toimintaa, mutta taustalla vaikuttavaa säätelymekanismia ei tunneta. 'Plasmalemma vesicle-associated protein' (PLVAP) on soluspesifinen endoteliaalinen kalvoproteiini, joka ilmentyy aukkoisissa ja ikkunallisissa kalvoissa osassa endoteelisoluja. Se säätelee verisuonten läpäisevyyttä, valkosolujen läpäisyä ja verisuonten muodostusta eri kudoksissa, mutta kiveksessä sen tehtävää ei ole vielä tutkittu.

Tämä väitöskirja koostuu neljästä eri tutkimuksesta: virtaussytometrisestä menetelmästä ja kolmesta muusta osatyöstä, joissa tutkimme USF1:n, RB/E2F3-vuorovaikutuksen ja PLVAP:n merkitystä kiveksen kehityksessä ja toiminnassa eri hiirimalleilla. Virtaussytometrinen menetelmä mahdollistaa nopean solukoostumuksen selvityksen tuoreesta tai viljellystä kiveskudoksesta. Toisessa osatyössä osoitettiin USF1:n ilmentyvän myös ituradan kantasoluissa, joissa se säätelee kantasolujen uusiutumisen ja erilaistumisen välistä tasapainoa. Kolmannessa osatyössä tutkittiin E2F3:n merkitystä kiveksen kehityksessä ja sen vuorovaikutusta RB:n kanssa aikuisen hiiren Sertoli solujen toiminnan ylläpitämiseksi. Väitöskirjan viimeinen osatyö osoitti PLVAP:n osallistuvan kiveksen kehityksen ja toiminnan hormonaaliseen säätelyyn.

AVAINSANAT: virtaussytometria, USF1, ituradan kantasolu, RB, E2F3, Sertolin solu, PLVAP

Table of Contents

Abbreviations

1C	haploid amount of DNA
2C	diploid amount of DNA
4C	tetraploid amount of DNA
A_{al}	type A-aligned spermatogonia
A_{pr}	type A-paired spermatogonia
ALCs	adult Leydig cells
AMH	anti-Müllerian hormone
ANOVA	analysis of variance
AR	androgen receptor protein
As	type A-single spermatogonia
Aundiff	undifferentiated spermatogonia
B	type B spermatogonia
BMP	bone morphometric proteins
BSA	bovine serum albumin
BTB	blood-testis barrier
CDK	cyclin-dependent kinase
CO2	carbon dioxide
DAPI	4´, 6-diamidino-2-phenylindole
DMEM	Dulbecco´s modified eagle medium
DNA	deoxyribonucleic acid
DNase	deoxyribonuclease
dpc	days *post coitum*
dpp	days *post partum*
DSB	double-strand break
E2F	E2 promoter targeting factor
E2F3a	E2F transcription factor 3 isoform a
E2F3b	E2F transcription factor 3 isoform b
FACS	fluorescence-activated cell sorting
FBS	fetal bovine serum
FOXL2	Forkhead box protein L2
FLCs	fetal Leydig cells

FSH	follicle-stimulating hormone
G1	Gap 1 phase of the cell cycle
G0	Gap zero phase of the cell cycle
GATA4	GATA binding protein 4
GDNF	glial cell line derived neurotrophic factor
hCG	human chorionic gonadotropin
IF	immunofluorescence
IHC	immunohistochemistry
LH	luteinizing hormone
mRNA	messenger RNA
p107	retinoblastoma-like 1
p130	retinoblastoma-like 2
PCR	polymerase chain reaction
PFA	paraformaldehyde
PGCs	primordial germ cells
PLVAP	plasmalemma vesicle-associated protein
PLZF	promyelocytic leukaemia zinc finger protein
pRb	retinoblastoma protein
PTM	peritubular myoid cells
qRT-PCR	quantitative RT-PCR
RA	retinoic acid
RB	retinoblastoma protein family
RNA	ribonucleic acid
RT	room temperature
SC-*Rb-/-E2f3-/-*	Sertoli cell-specific knockout of Rb and knockout of E2f3
SC-*Rb-/-E2f3+/-*	Sertoli cell-specific knockout of Rb and haploinsufficiency of E2f3
SC-*Rb-/-E2f3+/+*	Sertoli cell-specific knockout of Rb
SCs	Sertoli cells
shRNA	short hairpin RNA
SMA	smooth muscle actin
SOX9	SRY (sex determining region-Y) –box 9
SRY	sex determining region of chromosome Y
SSCs	spermatogonial stem cells
STRA8	stimulated by retinoic acid gene 8
TUNEL	terminal deoxynucleotidyl transferase dUTP nick end labeling
Usf1	upstream stimulatory factor 1

List of Original Publications

This dissertation is based on the following original publications, which are referred to in the text by their Roman numerals:

I   Rotgers, E*, **Cisneros-Montalvo S***, Jahnukainen K, Sandholm J, Toppari J, and Nurmio M. A detailed protocol for a rapid analysis of testicular cell populations using flow cytometry. *Andrology*. 2015, 3:947-955. (*equal contribution).

II   Faisal, I, **Cisneros-Montalvo S**, Hamer G, Tuominen MM, Laurila PP, Tumiati M, Jauhiainen M, Kotaja N, Toppari J, Mäkelä JA, and Kauppi L. Transcription Factor USF1 Is Required for Maintenance of Germline Stem Cells in Male Mice. *Endocrinology*. 2019, 160:1119-1136

III   Rotgers, E, **Cisneros-Montalvo S,** Nurmio M, and Toppari J. Retinoblastoma protein represses E2F3 to maintain Sertoli cell quiescence in mouse testis. *Journal of Cell Science*. 2019, 15:132

IV   **Cisneros-Montalvo, S.,** Lokka E, Nurmio M, Tyystjärvi S, Jokela H, Salmi M, Mäkelä JA, Toppari J and Rantakari P. Endothelial-specific plasmalemma vesicle-associated protein is needed for proper endocrine regulation of testicular development and function. *Manuscript.*

The original publications have been reproduced with the permission of the copyright holders.

1   Introduction

Infertility is a predominant condition that affects around 70 million people worldwide (around 0.9% of the whole population) [1]. According to the World Health Organization, 9% of couples worldwide struggle with fertility issues, with nearly 50% of the factors accounting for male defects [2]. The causes of male defects such as decreased sperm count or testicular dysfunction vary from chromosomal abnormalities to developmental alterations, lifestyle, endocrine disruptors, medical illnesses, and medications. Moreover, around 30% of the male infertility cases remain idiopathic [3].

Spermatogenesis (i.e., the production of spermatozoa) involves the proliferation, apoptosis, and differentiation of different somatic and germ cells in the seminiferous epithelium and interstitial space. This process is generally regulated by endocrine and autocrine/paracrine factors, which also include specific transcription factors.

In this thesis, we selected three important proteins that have been reported to play a role in different biological functions and have been indicated as a potential target for some abnormal conditions. However, very few studies have been performed on the reproductive function of these proteins. Therefore, using different mouse models, we revealed their role in testicular development and function. Upstream stimulatory factor 1 (USF1) is a ubiquitous transcription factor that has been shown to regulate multiple biological roles, such as synaptic plasticity, blood pressure, and glucose and lipid metabolism [4–6]. Moreover, as *Usf1*-deficient mice fed a high-fat diet (HFD) were found to exhibit a beneficial lipid profile, it has been suggested that USF1 can act as a potential therapeutic target for cardiometabolic diseases. However, the effects of *Usf1* deletion on male fertility have not yet been investigated. Retinoblastoma protein (RB) is a tumor suppressor protein that has been largely reported to control cell cycle, apoptosis, and differentiation [7]. We have previously reported that RB controls the function of Sertoli cells (SCs) in the adult testis [8]. Notably, *Rb* deficiency, specifically in SCs, compromises the maturation of SCs, impairing spermatogenesis. However, the molecular mechanism underlying RB role remains unknown. Plasmalemma vesicle-associated protein (PLVAP) is a transmembrane protein expressed in fenestrated vascular endothelia. This protein regulates vascular permeability, leukocyte migration, angiogenesis, and the seeding

of fetal liver-derived macrophages to different tissues [9,10]. It has been reported that *Plvap*-deficient mice exhibit barrier function and permeability failure, leading to the selective loss of plasma proteins. As the testicular vasculature consists of fenestrated endothelia, it is important to know the function of PLVAP in testicular development and function.

In the studies performed in this thesis, different mouse lines were used to reveal the important roles of the above-mentioned transcription factors in testicular development and function. Our data show that USF1 plays a critical role in the maintenance of spermatogonial stem cell (SSC) self-renewal and differentiation, that the RB/E2F3 interplay maintains adult SCs in a quiescent state, and that PLVAP plays a role in the endocrine regulation of the testis. Moreover, we developed a flow-cytometry-based method to study rodent testicular composition using intracellular fluorescent antibodies and DNA staining.

2 Review of the Literature

The testis is a paired endocrine and exocrine organ that assures the reproductive capacity and perpetuation of mammals. The principal functions of the testis are the production of androgens and the production of sperm. The following is a detailed description of testis development and function exclusively in mice, with few examples from human and rat.

2.1 Testicular development

Generally, the testis originates in the bipotential genital ridges, which are formed by the proliferation of the coelomic epithelium at 9 dpc (days *post coitum*) in mice or 28 dpc in humans during embryonic development [11,12]. At 10 dpc in mice, supporting cells, steroidogenic cells, and primordial germ cells (PGCs) develop, which originate from the yolk sac [13].

2.1.1 Male sex determination and fetal testicular development

Male sex determination includes the activation and suppression of specific genes for the organization and differentiation of the gonadal primordium (Figure 1). At 10–10.5 dpc in mice and 42 dpc in humans [14], a subset of supporting cells in the XY genital ridges transiently express the SRY gene [15,16]. These supporting cells engulf the PGCs, which then become gonocytes and form the sex cords. These supporting cells then become pre-SCs. The expression of SRY induces the expression of *Sox9* in mouse pre-SCs at 11.5 dpc, supported by positive-feedback loops with fibroblast growth factor 9 (FGF9), prostaglandin D2, and SOX9 itself. At the same time, these positive-feedback loops suppress the signaling of *Wnt*, *Rspo1*, and *Foxl2*, which are inducers of ovarian development [17].

When *Sox9* is upregulated, the mouse testis cord continues developing, including the shortening and thickening of the gonad until 14.4 dpc, at which loop-like structures are formed [18]. Other supporting and steroidogenic cells that are among and immediately juxtaposed at the periphery of the developing testis cords become fetal Leydig (FLCs) and peritubular myoid (PTMs) cells, respectively.

After the formation of the testis cords, masculinization of the fetus is promoted by the SCs and Leydig cells. Notably, SCs secrete anti-Müllerian hormone (AMH), which induces the regression of the Müllerian ducts [19], and support FLCs to produce testosterone for the development of the male reproductive tract and external genitalia [20]. Before birth, SCs actively proliferate, whereas gonocytes proliferate only until around 14.5–16.5 dpc in mice and then enter mitotic arrest [21,22]. In mice, the prevention of meiosis at this time point is achieved by the degradation of retinoic acid (RA) by CYP26B1 expressed by somatic cells in the testis, as well as by the expression of pluripotency-associated genes in the gonocytes [23–25].
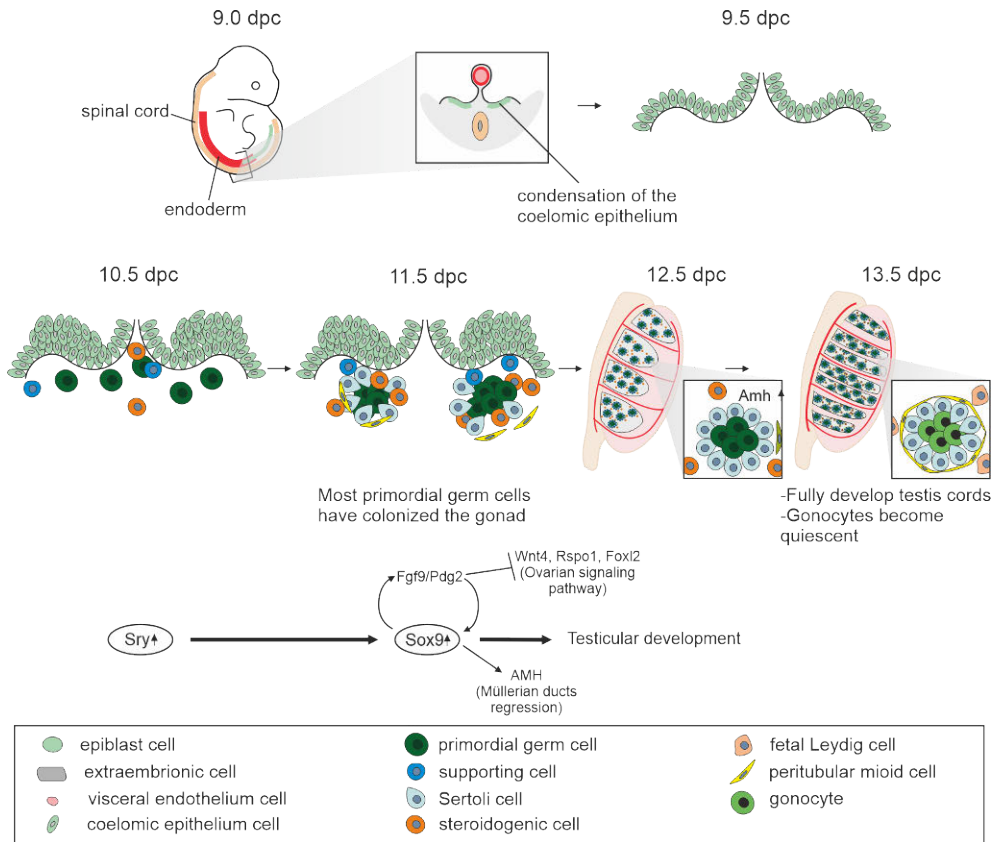
Figure 1. Overview of the process of male sex determination in mice. When the primordial germ cells (PGCs) arrive at the bipotential gonad at 10.5 dpc, at the same time, *Sry* is induced and the supporting cells reorganize and encapsulate the PGCs. By 11.5 dpc, the supporting cells start expressing *Sox9*, which suppresses the ovarian pathway and initiates the male sex determination pathway. Upregulation of Sox9 activates several male-specific genes for testicular development, including *Amh*, which regresses the Müllerian ducts. At 12.5 dpc, the testis cords form and the male morphological characteristics become evident. By 13.5 dpc, the testis cords become fully developed.

At 18.5 dpc, gonocytes begin to migrate to the basement membrane [26]. Generally, the molecular control of gonocyte migration has not yet been well characterized; however, it has been suggested that FGF signaling is the key regulator of gonocyte migration. Upon FGF signaling, the glial cell line-derived neurotrophic factor (GDNF) pathway is triggered, which in turn activates the mitogen-activated protein kinases (MAPK) and phosphatidylinositol 3-kinase (PI3K)/protein Kinase B (Akt) signaling pathways in these cells during gonocyte migration [27]. In addition, it has been reported that the stem cell factor (also known as KIT ligand) and platelet-derived growth factor (PDGF) secreted by SCs promote gonocyte migration [28–31]. After migration, the gonocytes become spermatogonia and can be identified through the expression of GFRA1 and cytoplasmic FOXO1 [27].

2.1.2 Postnatal testicular development

At birth, the testis cords develop into seminiferous tubules. In addition, germ cells reassume the cell cycle and SCs start actively proliferating (Figure 2). Gonocytes, now called spermatogonia, reassume the cell cycle at 1 dpp (days *post partum*) in mice [26], regulated by PDGF signaling [29,32]. Notably, some spermatogonia form the SSC pool [33], and another subset differentiate to participate in the first round of spermatogenesis. The first round of differentiation of spermatogonia usually takes place at 17 dpp when RA, synthesized by SCs, stimulates a subset of spermatogonia to express *Stra8* (stimulated by RA gene 8) and *cKit* (cellular homolog of feline sarcoma viral oncogene v-kit) and induce their differentiation [34]. Then, SCs stay at the basement membrane and continue actively proliferating until 17 dpp in mice [22]. After the gradual reduction in proliferation, the SCs differentiate into mature cells and form the blood–testis barrier (BTB). Each mature SC nurses a limited number of germ cells in the adult testis [35]; hence, the number of SCs reflects the size of the testis and the efficiency of sperm production.
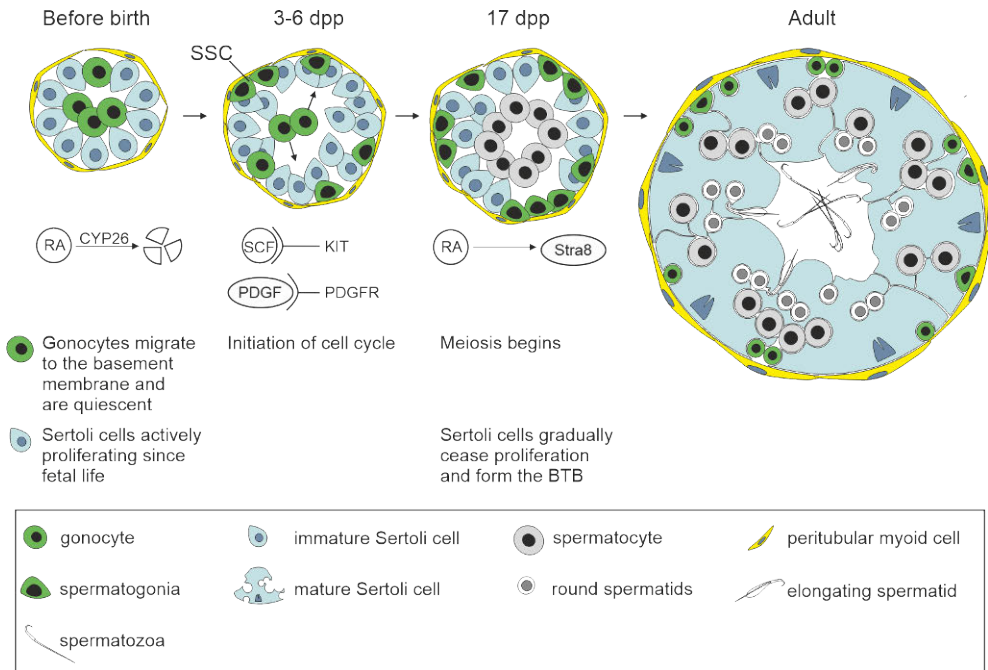
Figure 2. Postnatal testicular development in mice. Before birth, the gonocytes are maintained in a quiescent state because of the degradation of retinoic acid (RA) by CYP26, expressed in somatic cells. At this point, the Sertoli cells (SCs) are still actively proliferating. After birth, the gonocytes migrate to the basement membrane via the action of KIT and platelet-derived growth factor (PDGF) signaling. Once they reach the basement membrane, they become spermatogonia and reassume proliferation. By 17 dpp, RA induces the expression of *Stra8* in spermatogonia and meiosis begins, while SCs stop proliferating and form the blood–testis barrier (BTB). At the adult stage, the seminiferous tubules consist of germ cells in different steps of differentiation and quiescent SCs that nurse spermatogenic cells in every spermatogenic round.

2.2 Testicular composition

The testis consists of long coiled seminiferous tubules and an interstitial space between them covered by a fibrous envelope called tunica albuginea. These seminiferous tubules and the interstitial space host specific cell types essential for spermatogenesis. Spermatozoa migrate from the lumen of the seminiferous tubule to the rete testis and then move to the efferent ducts and the epididymis for further maturation.

2.2.1 Seminiferous epithelium

2.2.1.1 Spermatogonial stem cells and niche

Generally, SSCs are the precursors of all spermatozoa produced during the reproductive lifespan of a male. This cell population renews itself to maintain its number, and a subset of these cells become progenitor cells to enter the spermatogenic cycle (Figure 3). This fate decision is controlled by factors produced in a specific environment called the *niche*.

The *niche* of the SSCs is a three-dimensional environment that consists of the cells surrounding the SSCs and specific autocrine and paracrine factors. Over the years, different factors have been reported to affect the dynamics and function of SSCs. Among paracrine factors, GDNF, which is secreted by SCs, PTMs, and vascular endothelial cells, has been reported to be the most important factor for SSC self-renewal by blocking their differentiation [36–39]. Deletion of GDNF receptors causes the depletion of SSCs [40]. Conversely, its overexpression causes the accumulation of undifferentiated spermatogonia [37]. Fibroblast growth factor 2 (FGF2) also regulates SSC maintenance. Extended stimulation of FGF2 in the testis results in the accumulation of undifferentiated spermatogonia and represses the expression of the CYP26B1 enzyme to control RA [41]. Besides, several intrinsic factors in SSCs, such as promyelocytic leukemia zinc finger (PLZF) [42,43], TATA-box binding protein associated factor 4b (TAF4B) [44], spalt-like transcription factor 4 (SALL4) [45,46], and forkhead box O1 (FOXO1) [47], promote self-renewal and cell fate and survival.

In rodents, SSCs constitute a subset of a heterogeneous population of spermatogonia (type A, intermediate, and type B spermatogonia), which reside in the basement membrane of the seminiferous epithelium. Notably, the type A spermatogonia are further divided into an undifferentiated and a differentiated subpopulation. The undifferentiated subpopulation consists of A-single (A_s), A-paired (A_{pr}), and A-aligned (A_{al}) chains of 3 to 32 undifferentiated spermatogonia. According to the "A-single" model of spermatogonial differentiation [48], the SSCs are all A_s spermatogonia; however, recent studies have shown that A_s spermatogonia population consist of authentic SSCs, and SSCs in transition to a progenitor phenotype [49,50]. On the other hand, A_{pr} and A_{al} spermatogonia are progenitors cells connected by intracellular bridges formed after incomplete cytokinesis [51]. As a consequence of terminal differentiation, undifferentiated spermatogonia form A1 spermatogonia via RA induction [52]. A1 differentiated spermatogonia further divide mitotically to form A2 > A3 > A4 > intermediate > B spermatogonia > spermatocytes, before undergoing meiotic division.
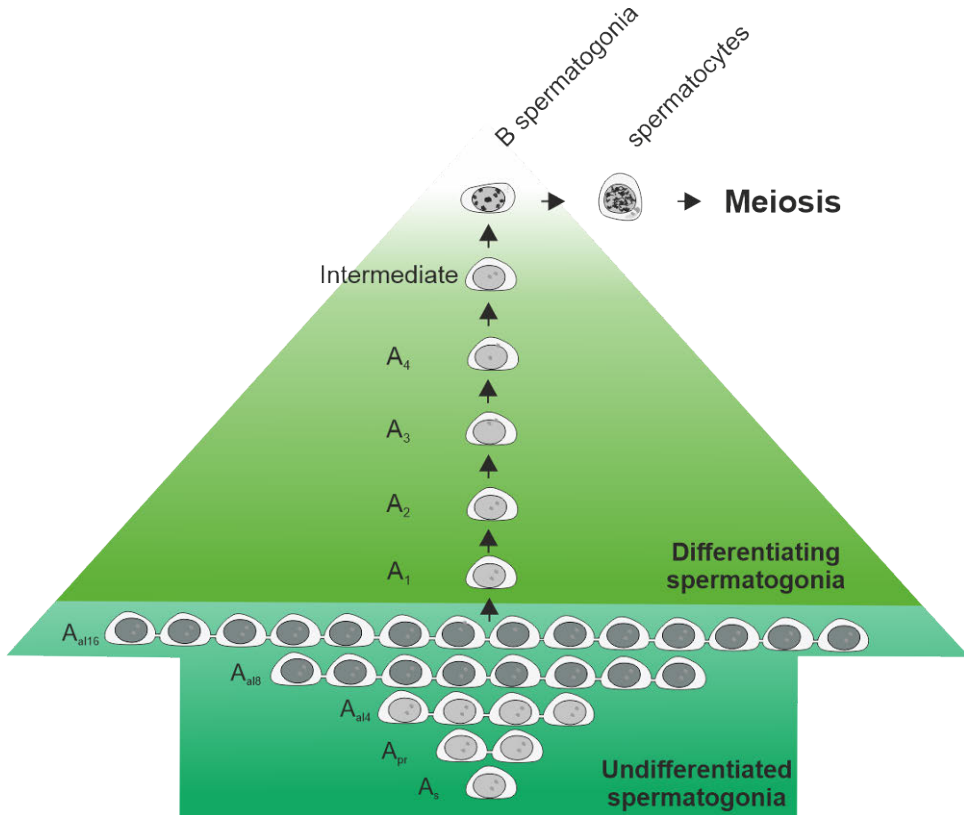
Figure 3. Formation of the spermatogonial stem cell syncytium in rodents. This process starts from the A-single (A_s) spermatogonia, which divide mitotically to give rise to A-paired (A_{pr}) spermatogonia. Mitotic division of A_{pr} spermatogonia produces A-aligned 4 (A_{al4}) spermatogonia and then A_{al8} and A_{al16} spermatogonia. All these cells constitute the undifferentiated spermatogonia. Unlike regular mitosis, cytokinesis in undifferentiated spermatogonia is incomplete. Therefore, these cells are connected to other cells via cytoplasmic connections. Undifferentiated spermatogonia transition into A1 as a commitment to spermatogenesis. They then divide (A1 > A2 > A3 > A4 > intermediate) and eventually form B spermatogonia, which then give rise to spermatocytes that undergo meiosis to produce haploid spermatids.

2.2.1.1.1 Spermatogenesis

Spermatogenesis is a synchronized and continuous process in which differentiation from diploid germ cells to haploid spermatozoa occurs. This process takes around 34 days in mice [1] and 74 days in humans [62] and is divided into three phases: mitotic amplification phase, meiotic phase, and postmeiotic phase of spermiogenesis.

During the *mitotic phase*, different subsets of undifferentiated spermatogonia proliferate or commit to spermatogonial differentiation, as described in the previous chapter. In theory, one committed spermatogonium can give rise to 2,048–4,096

spermatozoa by the end of the spermatogenic cycle [48]; however, several apoptotic mechanisms decrease the final output [49].

Preleptotene spermatocytes duplicate the amount of their DNA (4C) and proceed to *meiosis*. Spermatocytes first go through prophase I, which consists of six phases: preleptotene, leptotene, zygotene, pachytene, diplotene, and diakinesis. During these phases, the cell body and nucleus increase in size, sister chromatids condensate, the synaptonemal complex is formed, crossing over takes place, chiasmata become visible, and cells with recombined chromosomes split. This step involves different genes, such as *Rec8*, *Smc1b*, *Sycp3*, *Spo11*, *Dmc1* [50–54] and *Stra8* [55], as the earliest regulator of meiosis induced by RA signaling [56,57]. The first meiotic division is accomplished within metaphase I, anaphase I, and telophase I, resulting in cells called secondary spermatocytes with a 2C amount of DNA. During the second meiotic division, no DNA replication occurs and chromatids are segregated into two haploid cells (1C) called rounded spermatids (RSs).

During *spermiogenesis*, these RSs undergo morphological and structural changes to become spermatozoa. The cellular cytoplasm reduces, histones are replaced by protamines, and the formation of acrosomes and flagella takes place. Finally, mature spermatids are released to the lumen for further maturation in the epididymis [60,61].

2.2.1.1.2 Stages of the seminiferous epithelial cycle

The seminiferous epithelium consists of germ cells in different stages of differentiation. Classification of the epithelium according to the development of the acrosome of the spermatids forms highly defined associations called stages (Figure 4). The most undifferentiated cells are located next to the basement membrane. As the spermatogenic cycle proceeds, the most differentiated germ cells localize toward the lumen. In general, mice have 12 stages (I to XII) [62], rats have 14 (I to XIV) [63,64], and humans have 6 (I to VI) [65,66] or 12 [67], depending on the criteria.

As these stages take place progressively, each routine histological cross section of a seminiferous tubule can display one or two stages of the seminiferous epithelial cycle. Each stage displays a specific light absorption pattern (Figure 4), which allows the discrimination of specific stages in the seminiferous tubules under a microscope. Dissection of defined stages is very useful during toxicological and comparative analyses because it allows the evaluation of changes in cellular composition, biochemistry, and gene expression at each stage [64,68,69].
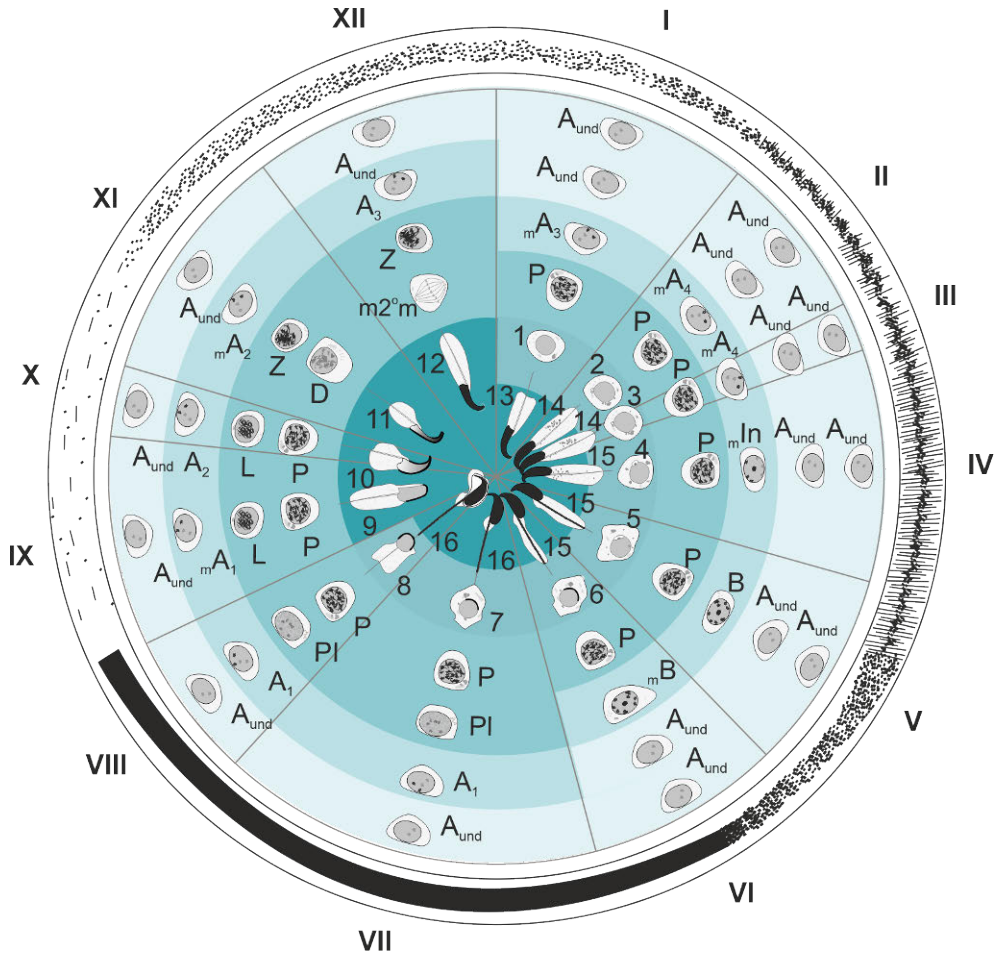
Figure 4. Cellular organization of the stages of the seminiferous epithelium in mice. The outer ring represents the transillumination properties of each spermatogenic stage. This clock contains all the cell types in each stage: A_{und}, undifferentiated spermatogonia; A_1, A_2, A_3, A_4, In, and B, differentiated spermatogonia; Pl, preleptotene spermatocytes; L, leptotene spermatocytes; Z, zygotene spermatocytes; P, pachytene spermatocytes; D, diplotene spermatocytes; m2°m, meiotic metaphase; 1–7, rounded spermatids (RSs); 8–16, elongated spermatids (ESs). The width of each stage represents the duration of one spermatogenic cycle [70].

2.2.1.2 Sertoli cells

Generally, SCs are the only somatic cells within the seminiferous epithelium that create a unique environment for nursing germ cells during spermatogenesis. These cells proliferate until two weeks in mice [22] or three weeks in rats [71] postnatally. By four weeks in mice and five weeks in rats, they acquire a mature quiescent status with cytoplasmic branches, BTB establishment, and the acquisition of the full capacity to sustain developing germ cells.

2.2.1.2.1 Sertoli cell proliferation

Proper proliferation of SCs determines the sperm production capacity of the testis as each SC can nurse a limited number of germ cells (Figure 5). Follicle-stimulating hormone (FSH) is the main regulator of SC proliferation during fetal and neonatal life. This hormone exerts its effects by interacting with the FSH receptor (FSHR) on the cell surface of the SCs. It has been widely reported that diminished FSH levels resulting from applying inhibitors or using transgenic models negatively affect the number of SCs [72–74].

Notably, AMH, a member of the transforming growth factor β (TGFβ) superfamily, mentioned in previous chapters, is expressed in SCs during the masculinization of the bipotential gonad to induce the regression of the Müllerian ducts. After birth, this expression decreases gradually until SCs become mature. Thanks to its expression pattern, AMH has been widely used as a distinctive marker for determining the status of SCs in rodents and humans [75,76].

Activin A is another member of the TGFβ superfamily that also regulates the proliferation of SCs during human and mouse fetal and postnatal testicular development. Activin A, a homodimer consisting of two β inhibin subunits (βA:βA homodimers) encoded by the *Inhba* gene, is produced by Leydig cells, SCs, and PTMs. During the fetal period, Leydig cells are considered the main source of activin A, whereas in neonatal life, PTMs are suggested to be the main source [77–79]. Generally, the levels of activin A become elevated during the proliferation of SCs and decrease as the animal reaches adulthood [79]. Complete deletion or specific deletion of *Inhba* in Leydig cells shows the importance of activin A for SC proliferation, as its deletion diminishes the number of SCs and results in a small-sized adult testis [78,80].

Interleukin-1 (IL-1) not only plays an important immunologic role but also plays a role in the proliferation of SCs. Generally, IL-1 exists as two major agonist isotypes, IL-1α, and IL-1β, which are both produced by SCs and Leydig cells in humans [81] and by interstitial macrophages in rodents [82–86].

2.2.1.2.2 Sertoli cell maturation

The acquisition of the full capacity of SCs to sustain spermatogenesis is mediated by different factors (Figure 5). It is widely known that testosterone functions in the virilization of the male embryo and progression of spermatogenesis in adults [20,88]. However, testosterone may also directly induce the maturation of SCs. Moreover, the androgen receptor (AR) is expressed in SCs, Leydig cells, and PTMs in the testis [89]. However, the expression in SCs starts postnatally and increases during postnatal testicular development, which correlates with the gradual cessation of SC

proliferation [90]. It has been shown that premature expression of AR in fetal SCs induces the maturation of SCs, which causes a reduce number of SCs and small-sized adult testis. Besides, gene expression analysis of SCs in this transgenic mouse model shows elevated mRNA levels of tight junctions and phagocyte-related function, demonstrating the premature maturation of SCs [91]. The upregulation of cyclin-dependent kinase (CDK) inhibitor 1B (p27Kip1) [92], which inhibits CDKs, ceases the proliferation of SCs. Inhibition of CDKs prevents the phosphorylation of RB, hence preventing the activation of cell cycle progression [93].

Triiodothyronine (T3) is a thyroid hormone implicated in the maturation of SCs. It has been suggested that the binding of T3 to its receptor in SCs induces the upregulation of Cx43, a constitutive protein of gap junctions that inhibits the proliferation of SCs. Besides, specific deletion of thyroid hormone receptor alpha 1 (TRα1) in SCs results in the increased proliferation of SCs with higher sperm production, whereas exposure of immature SCs to higher doses of T3 decreases their proliferation [94–96].

Another hallmark of SC maturation is the formation of the BTB. This barrier consists of tight junctions (formed by claudins 1–24, JAM 1–3, and ZO-1), an ectoplasmic specialization (formed by α1β6 integrin, ESPIN), a gap (formed by connexin 43), and desmosome-like junctions (formed by desmoglein, desmocollin, and vimentin) [97]. The BTB divides the seminiferous tubules into two compartments: a basal compartment, in which the SSCs and other spermatogonia are found, and an adluminal compartment, which consists of spermatocytes and spermatids. This complex structure maintains tissue homeostasis by protecting the developing germ cells from endo- or exogenous substances and autoimmune responses.

Mature SCs play a role not only during testicular development and spermatogenesis, but also during the last stage of spermiogenesis. In the last step of elongation, spermatids are still anchored to the branches of the SCs. When the residual body is released from elongated spermatids (ESs), SCs with a class B scavenger receptor type I recognize the phosphatidylserine exposed on the cell surface of the residual body and phagocytose it. It has been shown that impaired phagocytosis by SCs decreases the number of epididymal sperm [98]. Moreover, SCs are also important for the release of mature sperm to the lumen by modification of the apical ectoplasmic specializations [99].
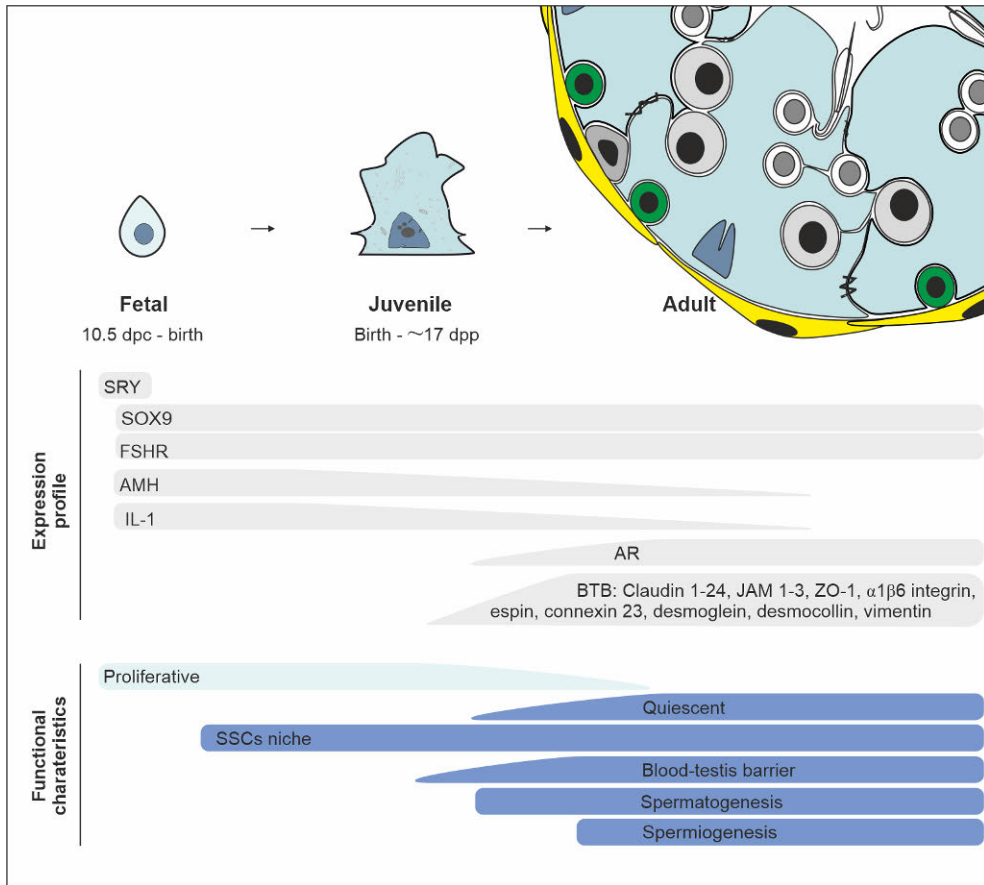
Figure 5. Sertoli cell (SC) differentiation in mice. During testicular development, SCs differentiate into fetal, juvenile, and adult SCs. Each phase is characterized by a specific expression profile and functional characteristics. Fetal SCs are first identified when precursor cells in the bipotential gonad start expressing SOX9 induced by SRY, which then induces male sexual differentiation of the testis. At the same time, the secretion of anti-Müllerian hormone (AMH) by fetal SCs induces the regression of the Müllerian ducts. At this point, the SCs express follicle-stimulating hormone receptor (FSHR) and interleukin-1 (IL-1) and actively proliferate. After birth, SCs support spermatogonial stem cell (SSC) niche formation and continue proliferating actively. At around 17 dpp, the SCs gradually cease to proliferate and start expressing AR and forming the blood–testis barrier (BTB). In the adult phase, the SCs differentiate into mature SCs and become mitotically quiescent somatic cells that can now support spermatogenesis.

2.2.1.3   Retinoblastoma and E2F protein families

2.2.1.3.1   Retinoblastoma protein family

The RB family consists of pRb, p107, and p130 mammalian proteins. These proteins are known to be transcriptional repressors because their major function is to inhibit

the expression of cell-cycle-related proteins [162]. Notably, pRb, p107, and p130 are considered to be closely related because they share a common pocket domain for interaction with viral oncoproteins and cellular factors, such as the E2F family. pRb is an RB that is ubiquitously expressed in adult tissues and is mutated in different types of human cancer, such as retinoblastoma, small-cell lung carcinoma, and osteosarcoma [163]. *p107* has been found to be mutated only in human B-cell lymphoma [164], whereas *p130* been found to be mutated in nasopharyngeal carcinoma [243] and lung carcinoma [244]. Despite the low-frequency mutation of *p107* and *p130* in human cancer, both of them contribute to some tumor suppressor functions in an *Rb* mutated background [165]. Moreover, these three members of the retinoblastoma family have some overlapping and opposing roles (for a review, see [166,167]).

2.2.1.3.2   E2F protein family

The E2F protein family includes eight genes, E2F1–E2F8, which encode nine proteins (because E2F3 has two products, E2F3a and E2F3b). According to the ability to activate or repress transcription, E2F proteins are divided into activators (E2F1, E2F2, and E2F3a), which are expressed during the G_1/S-phase, and repressors (E2F3b, E2F4–E2F8), which are expressed during the G_0/G_1-phase of the cell cycle (for a review, see [172]). All these E2F transcription factors are known to regulate the cell cycle progression and apoptosis [173,174]. Generally, E2F1–E2F5 activate or repress transcription by interacting with the RB protein family (pRb, p130, and p107). As E2F6–E2F8 lack sequences for binding to the Rb protein family, they perform their repression function by other mechanisms [175,176].

Despite the common domain that the RB protein family shares among its members, they interact differently with the E2F proteins. pRb interacts with E2F1 [177], E2F2 [178], E2F3 [179], and E2F4 [180], whereas p130 and p107 interact with E2F4 [181] and E2F5 [166,175,180]. These associations occur at different phases of the cell cycle. While pRb interacts with the E2F proteins in nondividing and dividing cells, p107 interacts primarily in nondividing cells and p130 interacts especially during the S-phase of the cell cycle [175].

Rb family members and cell cycle

Inhibition of cell cycle progression is achieved by blocking the transcriptional activity of E2F proteins. In quiescent cells, unphosphorylated RB forms complexes with E2F proteins to inhibit the activation of specific genes for cell cycle progression. When the cell becomes committed to divide, at the early G1-phase, cyclin/CDK complexes phosphorylate Rb. This disrupts the Rb/E2F association, causing the release of E2F, which then activates or represses target genes (Figure 6) [171].
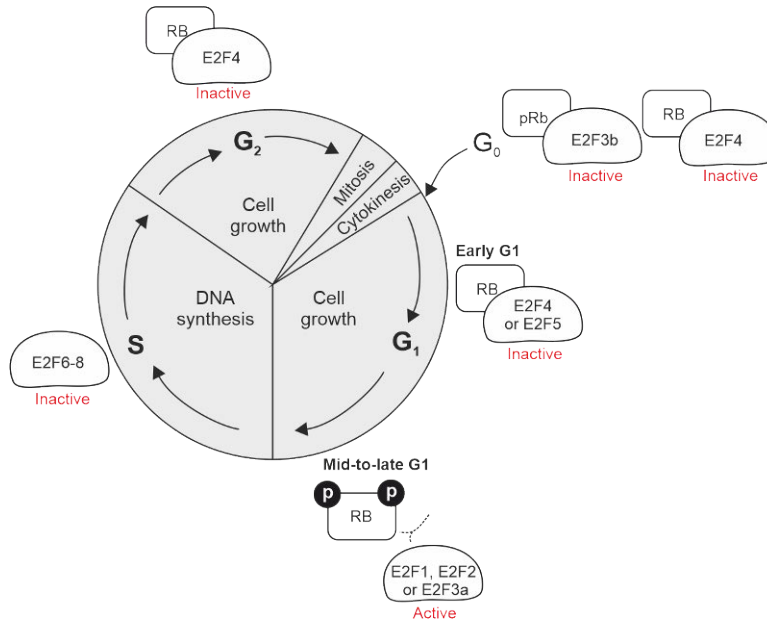
Figure 6. Retinoblastoma (RB) and E2F family proteins in the cell cycle. RB and pRb represent the unphosphorylated RB protein family member and the retinoblastoma protein, respectively, and **ⓟ** represents the phosphorylated forms. In the G_0- and early G_1-phases, RB physically associates with E2F factors and blocks their transactivation domain. In the late G_1-phase, phosphorylated RB releases E2F, allowing the expression of genes that encode products necessary for S-phase progression.

2.2.1.3.3 RB/E2F pathway in the testis

In the mouse testis, RB protein family and E2F transcription factors are expressed in different cell types and a stage-specific pattern. pRb is expressed in SC, dividing spermatogonia, and preleptotene spermatocytes, whereas p107 is expressed in meiotic spermatocytes and p130 is expressed in SCs [8,182]. Regarding E2F proteins, E2F1 is expressed in the leptotene to early pachytene spermatocytes of stages IX to XI in mice, as well as in the spermatogonia. E2F2 is expressed in the spermatocytes of the mid to late prophase of meiosis, E2F3 in SCs and differentiated spermatogonia, E2F4 in SCs, and E2F5 in B spermatogonia, preleptotene spermatocytes, and pachytene spermatocytes [8,183].

Using transgenic animals, different roles of the RB and E2F protein family have been indicated during spermatogenesis. Rb regulates the entry of gonocytes into cell cycle arrest in the fetal testis at 14.5 dpc. In *Rb*-null mice, the gonocytes do not enter cell cycle arrest and continue proliferating. Later on, the gonocytes achieve cell cycle arrest because of the compensatory effects of Cdkn1b and Cdkn2b [184]. In the germ cells, *Rb* insufficiency results in an impaired self-renewal capacity of SSCs (A_s) and the accumulation of progenitor spermatogonia (A_{al}). Consequently, the mice become

sterile as a result of the rapid exhaustion of the SSC pool [185]. On the contrary, *Rb* insufficiency in SCs induces cell cycle reentry of adult quiescent SCs. However, as SCs do not display a mature status, spermatogenesis fails [8,186].

Recently, we have reported that pRb and the E2F3 transcription factor are coexpressed in mouse SCs and that they mediate SC maturation and cell cycle quiescence [8]. E2F1 has been linked to the induction and inhibition of apoptosis in the testis. Ablation of E2F1 in different genetic backgrounds has been shown to cause the disruption of spermatogenesis [187,188]. A later study showed that E2F1 promotes the apoptosis of spermatogonia during the first wave of spermatogenesis and inhibits the apoptosis of meiotic germ cells [188]. Besides, E2F1 may also regulate the function of SCs and induce their apoptosis in the absence of Rb [186].

Notably, the testis phenotype of *E2f2*-null mice has not yet been studied. However, studies on the immunological functions of E2F2 have described that *E2f2*-null mice are viable and fertile and produce normal offspring, which may suggest that E2F2 is not essential for spermatogenesis [245]. E2F3 protein expression has been reported in Sertoli and spermatogonia cells [183]. However, to our knowledge, this is the first study investigating the protein expression of E2F3 isoforms and their function in the SC of the mice testis. *E2f4*-null mice die at birth as a result of respiratory system infections, challenging the study of E2F4 in spermatogenesis [189]. Treating the mother with antibiotics can generate *E2f4*-null littermates that survive until adulthood. These *E2f4*-null mice are infertile. Surprisingly, no phenotype was seen in the adult testis, but in the epididymis, which may suggest that E2F4 is dispensable for spermatogenesis but essential for epididymal function [189]. This result is in line with the notion that E2F4 and E2F5 may have overlapping functions, which may be the reason for a normal testis phenotype [190]. Besides, mice with double deletion of E2F4 and E2F5 are not viable and die *in utero* [180]. Generally, E2F6 is dispensable in cell cycle progression or inhibition in the testis; however, it has been reported that E2F6 represses the expression of meiosis-specific genes in somatic cells [191].

As mentioned above, some RB and E2F proteins compensate for the absence of other proteins in terms of function. However, more studies need to be performed to determine the compensatory and specific roles of each protein or complex (RB/E2F) in the testis.

2.2.1.4   Upstream stimulatory factor 1

Upstream stimulatory factor 1 is a general ubiquitously expressed transcription factor that plays many roles in biological systems, such as glucose and lipid metabolism [148,149]. However, the expression of USF1 and its ability to regulate spermatogenesis is still poorly characterized.

Generally, USF1 belongs to the basic helix-loop-helix family of transcription factors. Moreover, USF proteins are encoded by *Usf1* and *Usf2* genes. To regulate

transcription, the USF1 homodimer or USF1/USF2 heterodimer binds specific DNA sequence motifs known as E-boxes (CACGTG or CANNTG) in the target genes [145,146]. The first role identified for USF1 is the potential activation of the adenovirus major promoter in HeLa cells [147]. Later on, USF1 has been linked to lipid and glucose metabolism as it targets specific genes, such as L-type pyruvate kinase, fatty acid synthase, and glucokinase [148,149]. Besides, several genome-wide linkage scan studies have strongly linked *Usf1* to familial combined hyperlipidemia [5,150], coronary atherosclerosis [151,152], and acute cardiovascular events [153,154]. Moreover, different clinical studies have associated gene variants of *Usf1* to type 2 diabetes, metabolic syndrome, and obesity [155–157].

It has been reported that *Usf1*-deficient mice in different hybrid backgrounds are phenotypically normal, healthy, and fertile [159,246,246]. This normal phenotype has been suggested to be due to the compensatory effects of USF2 because its level is elevated in *Usf1*-deficient mice [159]. Laurila *et al*., [6] reported that *Usf1*-deficient mice fed with an HFD display a beneficial metabolic phenotype in comparison to control mice on HFD. They also display lower-body fat weight gain than that of the control animals on HFD and exhibit increased brown adipose tissue activity, elevated high-density lipoprotein cholesterol, decreased triglyceride level in plasma, and improved insulin sensitivity, suggesting that the inactivation of USF1 protects mice against diet-induced dyslipidemia, obesity, insulin resistance, and hepatic steatosis. Therefore, it has been proposed that USF1 can be used as a potential drug target for cardiometabolic diseases [6].

In the testis, USF1 has been identified as a potential regulator of SC differentiation, as *Usf1* mRNA and USF1 protein are upregulated in SCs at around 11 dpp in rats, corresponding to the maturation of SCs in rats [146]. Several *in vitro* studies have indicated that the DNA-binding activity of USF1 to *Fshr*, *Gata4*, *Nr5a1* (also known as SF-1), and *Shbg* (also known as androgen-binding protein) promoters increases in the SCs of rats at 11 dpp [146,160]. Besides, in another study, it has been indicated that USF1 may also regulate *Fshr* transcription specifically in differentiating SCs as it actively binds the promoter of *Fshr* in differentiating SCs in mice and rats. Despite the strong binding capacity, the testes of *Usf1*-deficient mice at 21 dpp of age did not display any differences in the *Fshr* mRNA levels in comparison to wild-type (WT) mice [161,247], which could be the result of a compensatory function by *Usf2*.

2.2.2   Interstitial space

2.2.2.1   Testicular vasculature

In general, the testicular vasculature (i.e., blood and lymphatic vasculature) is formed during fetal testicular development simultaneously with the expression of SRY and

the formation of the testis cords [100,101]. Abnormal development of the testicular vasculature leads to intratesticular hypoxia and germ cell apoptosis [102].

In the adult, the testis is irrigated by three vessels (Figure 7), testicular, cremasteric, and deferential arteries, among which the testicular artery is the principal source. This testicular artery, which originates from the abdominal aorta, courses along the surface of the testis and then traverses the tunica albuginea and branches into a complex network of capillaries that travel among the seminiferous tubules [103]. The veins emerging from the testis form a conglomerate called the pampiniform plexus, which transports the drained blood from the testis, epididymis, and vas deferens and also regulates the temperature of the testis.

This complex vasculature provides a path for delivering pituitary hormones, micronutrients, and oxygen to the interstitial space among the seminiferous tubules. It also transports intratesticular testosterone (ITT) and helps get rid of it from the testis. The transfer of particles from plasma to the interstitial space depends on the vascular permeability and blood flow. Blood flow is positively correlated with the serum testosterone level and testis volume [104]. Testosterone, via AR in the smooth muscle cells of the vasculature, mediates testicular vasomotion [105,106], which is important for proper interstitial fluid homeostasis in the testis.
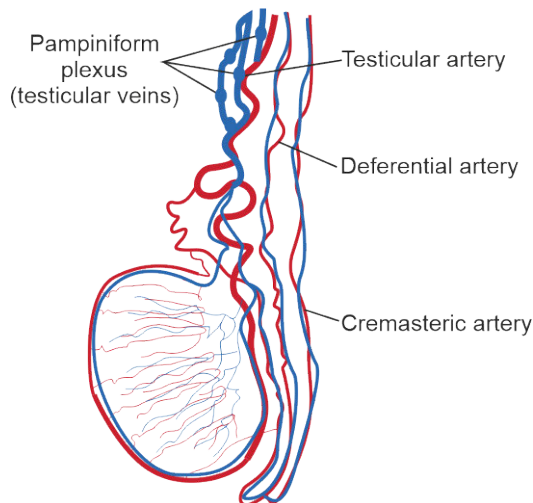

Figure 7. Testicular vasculature. The testis is irrigated by three arteries—the testicular, deferential, and cremasteric arteries—which deliver micronutrients, hormones, and oxygen to the testis. The testicular veins then collect waste and direct the testosterone out of the testis.

2.2.2.1.1 Endothelial cells

Endothelial cells line blood and lymphatic vessels and are known to regulate permeability, passive diffusion, active transport of molecules, and control of vasodilatation of the vasculature. In terms of morphology, endothelial cells are classified as continuous, discontinuous, or fenestrated endothelia, with each type differing in the organization of the endothelial cells and permeability. The testis consists mostly of fenestrated endothelia, which are characterized by the presence of transcellular pores with a diameter of around 60–80 nm [107], which allow the transport of macromolecules and migration of cells. These pores consist of a diaphragm that acts as a filter. So far, the only protein described forming the diaphragm is PLVAP [9].

In the adult testicular vasculature, similar to SCs and PTMs, endothelial cells produce GDNF under androgen stimulation, which regulates SSC homeostasis [1–4].

2.2.2.2 Plasmalemma vesicle-associated protein

Generally, PLVAP is a glycosylated type II transmembrane protein expressed in the diaphragm of fenestrated endothelia (i.e., fenestrae, caveolae, and transendothelial channel subcellular organelles), which line the inner surface of the microvasculature [192]. The expression of PLVAP is specifically localized to the diaphragm and is crucial for its formation. Moreover, this protein is not expressed in the endothelial cells of large vessels except in the endocardial lining of the heart chambers [193]. As it has been shown that this protein is expressed only in endothelial cells, it has been widely used as a blood endothelium specific marker.

Notably, PLVAP is important for the integrity of blood vessels and barrier function. Several *in vivo* and *in vitro* studies have demonstrated that PLVAP is responsible for the formation of diaphragms in caveolar and fenestral subcellular organelles [9,192]. It has also been observed that *Plvap*-null mice with a C57BL/6N genetic background die before birth because of subcutaneous edema, hemorrhages, and defects in the vascular wall of subcutaneous capillaries [194]. In a mixed background, *Plvap*-deficient mice can survive for a few weeks after birth [9,194], but they die soon because of severe enteropathy and edema of the intestine, kidneys, and pancreas. Lack of PLVAP in the endothelium impairs the barrier function, causing a massive leakage of molecules and plasma proteins [9].

It has also been shown that PLVAP regulates the traffic of immunological cells. Several *in vitro* and *in vivo* studies have shown that PLVAP mediates the traffic of lymphocytes into the lymph nodes [195]. In addition, PLVAP regulates the seeding of fetal liver-derived macrophages to different tissues [10].

In cancer, PLVAP was first detected in malignant glioma microvasculature [196]. Then, it was shown that PLVAP is upregulated in different kinds of cancer, such as lung, colon, liver, pancreas, ovarian, brain, and breast cancer [196-198]. Moreover, PLVAP is upregulated in primary and metastatic types of cancer, colocalizing with the CD31 antigen, a widely used marker for vascular endothelia [199]. It has also been shown that PLVAP promotes angiogenesis and growth of cancer cells. Several *in vitro* studies have shown that targeting PLVAP yielded positive results in terms of decreasing the size of tumors [200,201], allowing it to be considered a novel drug target for the treatment of cancer [196,202].

Apart from cancer, PLVAP has been identified in other diseases, such as acute ischemic brain disease, in which the blood–brain barrier is damaged, increasing the permeability of the microvasculature and, hence, leading to brain ischemia, hypoxia, and eventually mortality. Moreover, it has also been found that PLVAP is upregulated in part of the endothelial cells close to the ischemic area and, hence, is suggested to cause hypoxia [202]. After traumatic spinal cord injuries, expression of PLVAP is observed in newly formed blood vessels. Upregulation of PLVAP is thought to induce inflammation and deterioration of neurovascular function in this area [203].

The testicular vasculature consists mostly of fenestrated endothelia. Although PLVAP mRNA has been detected in the testis [204], its protein expression is still unclear. Immunohistochemical staining of the testes of newborn rats revealed the presence of PLVAP in the interstitial space between the seminiferous tubules. However, the same study that reported this finding also claims that, in the adult rat testis, PLVAP is not expressed in the interstitium but in the germ cells [204]. Nevertheless, the functional role of PLVAP in the testis remains unknown.

2.2.2.3   Leydig cells

Leydig cells are the steroidogenic cells of the testis that regulate the production of testosterone for the formation of the male genitalia and the production of sperm in the adult stage. Two populations of Leydig cells have been identified in mammals: FLCs and adult Leydig cells (ALCs) [109]. Although their developmental origin is still a matter of controversy, it is understood that each population derives from different progenitor populations in fetal life. Generally, FLCs are first identified at 12.5–13.5 dpc in rodents and increase in number during fetal life [110,111]. At birth, the mouse FLC population starts gradually atrophying, and at around 11 dpp, ALCs start populating the testis [112]. By 56 dpp, the percentage of FLC drops to around 20% only of the total Leydig cells [113]. During fetal life, FLCs cannot synthesize testosterone because they do not express 17β-hydroxysteroid dehydrogenase type 3 (17β-HSD3); they only secrete androstenedione, which is converted into

testosterone by fetal SCs that express 17β-HSD3 [113,114]. Notably, the function of the remaining FLCs in the adult testis is still unclear. However, ALCs express 17β-HSD3 and can synthesize testosterone following luteinizing hormone (LH) stimulation.

2.2.2.4   Peritubular myoid cells

Generally, PTMs are thin smooth-muscle-like cells that surround the seminiferous tubules. Although these cells can be identified in the testis at 13.5 dpc in mice [125], their origin remains unclear. These cells regulate postnatal testicular growth [126] and provide physical support and contraction of tubules in the adult testis for the release of mature spermatozoa to the epididymis [127]. Besides, PTMs are regarded as structural cells because they secrete components of the intercellular matrix, such as collagens (I, VI, and XVIII), laminin, and fibronectin [128]. According to an *in vitro* study, GDNF secretion induced by testosterone in PTMs regulates the maintenance of SSCs [129].

2.2.2.5   Macrophages

Macrophages are the most abundant cell population of the immune system in the adult testis [115–117] with various functions in different organs, such as an immunologic function, a tissue homeostatic function, and a regenerative and developmental function [118–120]. In the adult testis, two populations of testicular tissue-resident macrophages have been identified in terms of tissue localization, morphology, and gene profile. The macrophages situated in contact with Leydig cells, which display an immunosuppressive profile, have been suggested to play a role during postnatal Leydig cell development, regeneration, and steroidogenesis [120,121], whereas the macrophages situated in close contact with PTMs, which highly express genes for antigen processing and presentation, have been suggested to regulate the differentiation of SSCs [122].

It has been reported that testicular tissue-resident macrophages have a dual origin: the yolk sac (during the embryonic period) and the bone marrow (postnatally) [122]. It has also been suggested that macrophages localized close to Leydig cells have an embryonic origin [123], whereas those close to PTMs may have originated postnatally from the bone marrow [124].

2.3 Endocrine regulation of testicular function

In normal testicular development, male hormone secretion, and spermatogenesis are regulated by the hypothalamic-pituitary-gonadal axis (Figure 8). The hypothalamus secretes gonadotropin-releasing hormone, which induces the secretion of LH and FSH from the gonadotrophic cells in the anterior pituitary. Then, LH and FSH stimulate the testis, which in turn secretes testosterone by Leydig cells and inhibin B by SCs [131]. This mechanism sustains closed-loop feedback that maintains a balance of serum levels of reproductive hormones.

Previously, it has been believed that spermatogenesis is maintained by a high concentration of ITT, 50 to 100 times higher than in serum. However, in the last 10 years, transgenic mice models and clinical cases have provided new information regarding the hormonal need for spermatogenesis. In 2001, Zhang et al. [135] described the testicular phenotype of a mouse model lacking the LH receptor (LuRKO). Notably, LuRKO mice showed a small-sized testis and at six weeks of age displayed spermatogenic arrest around the spermatid stage. Hormone measurements revealed that the FSH level was twofold higher in serum and that the ITT levels were significantly reduced in LuRKO compared to WT mice, explaining the spermatogenic defect. However, at 12 weeks of age, the LuRKO mice displayed complete spermatogenesis, raising the question of whether the significantly low quantities of testosterone or the twofold higher FSH levels in the LuRKO mice were the underlying factors maintaining spermatogenesis. Moreover, antiandrogen treatment with flutamide blocked the progression of spermatogenesis in the testes of LuRKO mice and revealed that low ITT levels can drive spermatogenesis.

Different transgenic animals studying the function of FSH in spermatogenesis have supported the function of FSH on the proliferation of SCs and therefore the testis size [73,130]. Mice deficient in FSH-specific β subunit (FSHβKO) [240] and FSHR (FSHRKO)[133,239] display small-sized but fertile testes with normal spermatogenesis. Therefore, FSH is not essential for spermatogenesis.

In 2018, Odewule et al. [134] crossed a mouse line with an active mutation of FSHR in SCs, with an absent testis phenotype, together with LuRKO mice. Animals with strong FHSR stimulation and without testosterone were found to display normal spermatogenesis. Double knockout mice were treated with antiandrogen flutamide to eliminate possible testosterone action; however, no effect on spermatogenesis was observed, suggesting that the overactivation of FSHR can compensate for the AR action. Despite the different mechanism of action of FSHR and AR, both can activate the MAPK and CREB signaling pathway as a nonclassical testosterone pathway [248], which may explain how a strong FSH action can compensate for the absence of ITT for normal spermatogenesis.
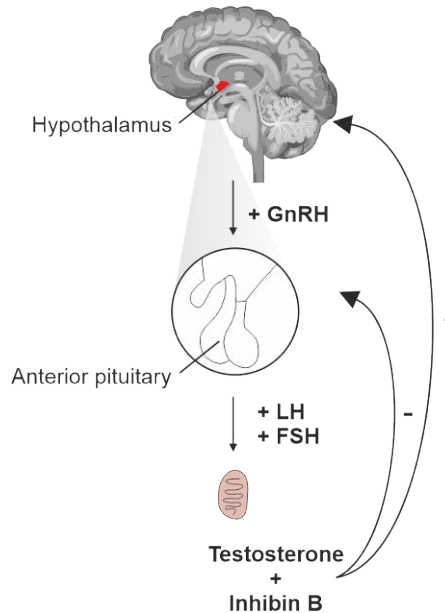
Figure 8. Schematic representation of the hypothalamic-pituitary-testicular axis. GnRH, gonadotropin-releasing hormone; LH, luteinizing hormone; FSH, follicle-stimulating hormone.

2.4 Morphometric methods to study testicular cell dynamics

The testis is a complex organ that consists of a heterogeneous population of germ cells and somatic cells. The proportion of each testicular population fluctuates during the fetal, juvenile, and adult stages. Besides, the cellular shape, size, and organization of the seminiferous tubules vary according to the stage of spermatogenesis, thus making the study of the testis challenging. Traditionally, standard hematoxylin and eosin or periodic acid–Schiff staining is performed on cryopreserved or paraffin sections for simple histological assessments. Then, photos are taken using conventional microscopes or, currently, automated scanners; however, the quantification of specific cell types is performed manually most of the time. Detection of specific cell types using immunohistochemistry or immunofluorescence techniques helps in the identification and quantification of cells of interest; however, this process can take days or even weeks.

2.4.1 Flow cytometry for the study of testicular dynamics

Flow cytometry is a laser-based technology that was first introduced in the 1950s to detect and measure the number and physical characteristics of cells in suspensions.

Currently, modern flow cytometers coupled to immunofluorescence and cell-sorting equipment allow researchers to perform multiparameter analysis for single cells to investigate parameters such as cell cycle, apoptosis, and even molecular pathways. When a single-cell suspension is injected into a flow cytometer, the cells become aligned thanks to the hydrodynamic focusing properties created by the outer sheath fluid in the flow cytometer (Figure 9). This single line of cells passes through a nozzle to a laser beam one cell at a time. As the cells pass through the laser beam, forward- and side-scattered light are collected using detectors, and the fluorescent light emitted from stained cells is also collected. The direction of the forward- and side-scattered light correlates with the size and granularity of the cells, respectively (Figure 8).

In the field of reproduction, flow cytometry coupled to DNA staining is performed to identify the status of spermatogenesis in rodents and primates [137–140] as well as in the human testis [141]. Incorporating DNA stains, such as propidium iodide, Hoechst stain, or fxCycle, allows the identification of testicular populations according to the amount of DNA. If the testis belongs to a juvenile rodent, two main populations can be identified: (1) a 2C population with double the amount of DNA, consisting of spermatogonia in the G_0/G_1-phase of the cell cycle and nonproliferative somatic cells, and (2) a 4C population with quadruple the amount of DNA, consisting of spermatogonia and somatic cells in the G_2/M-phase of the cell cycle and meiotic spermatocytes. Unlike in juvenile rodents, the testis of adult rodents consists of 2C, 4C, and 1C populations. Several defined stages of the epithelial cycle of mice and rats have been characterized using flow cytometry coupled to DNA staining, enabling the study of the dynamics among the different stages and their further use in toxicological studies [138,139].

Despite the accurate quantitative information that DNA staining provides, the 2C, 4C, and 1C populations are very heterogeneous populations consisting of germ and somatic cells. To resolve this inconvenience, fluorescent antibodies have been coupled to flow cytometry. Fluorescent cell-surface antibodies are applied to fresh cell suspensions [39,124,142] and intracellular antibodies are applied after the single-cell suspension is fixed and permeabilized [142]. However, the availability of different cell-surface markers for testicular cells and the optimization of intracellular antibodies are the main challenges in this technique. Additionally, normalization of large-scale data has not yet been well established [143,144].
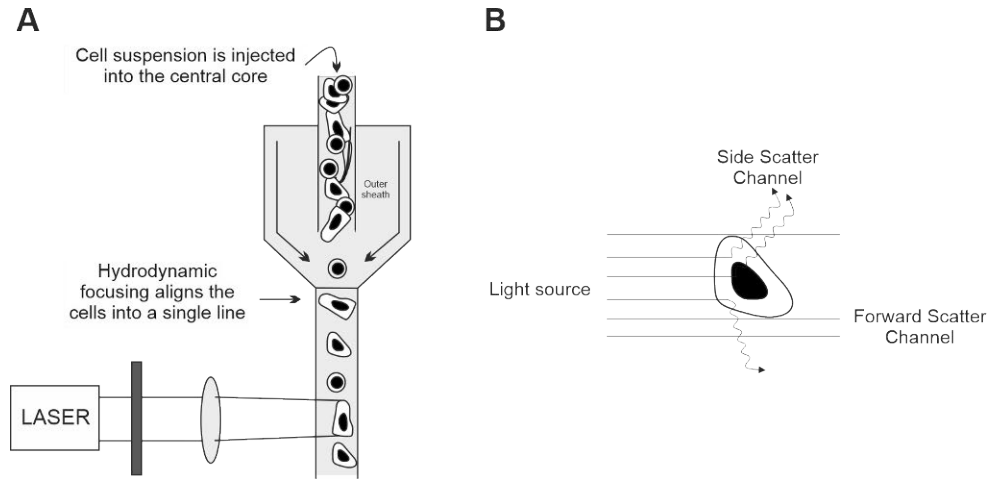
Figure 9. Basics of flow cytometry. (A) When a single-cell suspension is injected into the flow cytometer, it is transported to the sheath. The outer sheath applies pressure to the cells and, through hydrodynamic focusing, forces the cells to move as a single-file stream of cells to the laser beam region. (B) When the laser illuminates the cell, light scatters depending on the physical properties of the cell. Notably, forward- and side-scattered light correlate with the cell size and granularity of the cells, respectively.

3   Aims

The main objective of this study is to reveal the function of the transcription factor USF1, the transcription factor E2F3 alone or in combination with pRb, and PLVAP in the development and function of the testis. To facilitate the quantitative analysis of the testicular composition, a flow-cytometry-based method was developed.

The specific objectives of this study are as follows:

I.   To develop a flow-cytometry-based method to quantitatively analyze the testicular cell composition and dynamics of rodents.

II. To uncover the role of USF1 in the development and function of the testis using a USF1 KO mouse model.

III. To study the function of E2F3 and its interaction with pRb in the maintenance of adult SC function by developing SC-specific mouse models.

IV. To study the role of PLVAP during testicular development and function using a PLVAP KO mouse model.

4 Materials and Methods

Complete information on the catalog codes of the reagents used is provided in the original publications (I–III) and the manuscript (IV).

4.1 Experimental animals and treatments (I–IV)

Sprague Dawley rats were obtained from the animal facility of the University of Turku and used in Study I, whereas transgenic mouse lines were used in Studies II, III, and IV. Briefly, a $Usf1^{-/-}$ mouse line was produced from embryonic stem cells deficient in $Usf1$ from the German Gene Trap Consortium (clone M121B03). (II) Amh-cre[Plekha5Tg(AMH-cre)1Flor] [205], Rb-floxed (FVB;129-Rb[1tm2Brn/Nci]) [206], and $E2f3$-floxed ($E2f3$[tm1.1Gle]; generously provided by Professor Gustavo Leone, Ohio State University) [207] were crossbred to obtain Amh-cre[+]$E2f3$[flox/flox] (SC-E2f3KO) and Amh-cre[+]Rb[flox/flox]$E2f3$[flox/flox] (SC-RbKO$E2f3$KO) selectively in SCs. (III) Young and adult Plvap[tm1Salm] ($Plvap^{-/-}$) male mice were obtained from Adjunct Professor Pia Rantakari, Turku Bioscience Centre, University of Turku, and Åbo Akademi University.

All animals were housed under environmentally controlled conditions (12 h light/12 h dark, temperature: $21 \pm 1°C$). Animals in Studies I, III, and IV were fed with SDS R3 (Special Diet Services, E, Spy-free, Whitman, Essex, UK) *ad libitum* and housed in the animal facilities of the University of Turku. On the other hand, animals in Study II were fed with Teklad 2916 (Envigo; Indianapolis, IN, USA) *ad libitum* and housed at the Laboratory Animal Center of the University of Helsinki.

All procedures performed in this study followed the institutional and ethical policies of the University of Turku (Studies I, III, and IV) and the University of Helsinki (Study II) and were approved by the local ethics committees for animal experimentation.

4.2 Isolation of stage-specific segments of seminiferous tubules (II)

Seminiferous tubule segments of stages II–V, VII-VIII, and IX–XI were dissected from adult mouse testes using a transillumination-assisted microdissection method [64,68]. All seminiferous segments were snap-frozen in liquid nitrogen and stored at −80℃ for further gene analysis.

4.3 Gene expression analysis (II–IV)

4.3.1 PCR (II–IV)

Genotyping of the mouse lines was performed from ear (III–IV) or tail (II) pieces. DNA was isolated and PCR was performed as described previously [6,8,195,205–207]. The primers for *Usf1* genotyping in Study II were primer A (5′-GGCGCAGTGGTACTGGAGAGGA-3′), primer B (5′-ACCCCAAACCCAGGCGGCA-3′), and primer C (5′-TGACGCGCCGCTGTAAAGTGTTA-3′), which amplify 457 and 167 bp fragments for the KO and WT allele, respectively. To confirm the Cre expression for Amh-Cre in Study III, primer Cre26 (5′-CCTGGAAAATGCTTCTGTCCG-3′) and primer Cre36 (5′-CAGGGTGTTATAAGCAATCCC-3′) were used, which amplify a 400 bp fragment. For the *Rb* flox allele, primer *Rb*P1 (5′-GGCGTGTGCCCATCAATG-3′) and primer *Rb*P2 (5′-AACTCAAGGGAGACCTG-3′) were used, which amplify 700 and 650 bp fragments for the *Rb*-floxed and *Rb*-WT allele, respectively. For the *E2f3* flox allele, primer A (5′-GTGGCTGGAAGGGTGCCAAG-3′), primer B (5′-TGAATCATGGACAGAGCCAGG-3′), and primer C (5′-GATTGATTCTGGGTTGTCAGG-3′) were used, which amplify 250 and 200 bp fragments for the *E2f3*-floxed and *E2f3*-WT allele, respectively. In Study IV, primer A (5′-GTACATGCAACACCACTGAGC-3′), primer B (5′-CCTTGACAGGTGATGTCTGC-3′), and primer C (5′-AGTGTATGCTACCACATCTGGCTC-3′) were used, which amplify 1,100 and 210 bp fragments for the KO and WT allele, respectively.

4.3.2 Quantitative reverse transcription PCR (II)

Total RNA from the whole testis was isolated using a NucleoSpin RNA extraction kit (Macherey-Nagel, Duren, Germany), and RNA from stage-specific seminiferous tubules was isolated using TRIzol (Thermo Fisher Scientific, Waltham, MA, USA),

according to the manufacturer's instructions [8]. cDNA synthesis and quantitative reverse transcription PCR (RT-qPCR) were performed using the SsoAdvanced Universal SYBR Green Supermix (Bio-Rad Laboratories, Hercules, CA, USA) following the manufacturer's instructions. Primers were selected from our previous studies [8] or designed using Primer3-based software. Gene expression was normalized to housekeeping genes (α-tubulin and Wilms tumor 1 [WT1]) using the Bio-Rad CFX Manager software version 3.1 (Table 1).

Table 1.   Primers used for quantitative reverse transcription PCR (RT-qPCR).

Gene	Amplicon size (bp)	Forward primer (5´-3´)	Reverse primer (5´-3´)
Actb	216	AGACTTCGAGCAGGAGATGG	AGGTCTTTACGGATGTCAACG
Amh	149	GCTAGGGGAGACTGGAGAAC	CTGGTCCAGGGTATAGCACT
Ar	169	TACGGAGCTCTCACTTGTGG	CCAGAGTCATCCCTGCTTCA
Bmp4	182	AGGAGGAGGAGGAAGAGCAG	CACCTCATTCTCTGGGATGC
Ck18	167	TGACACCAACATCACAAGGC	TGAGGTCCTGAGATTTGGGG
Csf1	160	CTGCAGCAGTTGATCGACAG	GGGTGTTGTCTTTAAAGCGC
Cxcl12	126	TGCATCAGTGACGGTAAACC	CTGAAGGGCACAGTTTGGAG
Fgf2	104	GCGACCCACACGTCAAACTA	CCGTCCATCTTCCTTCATAGC
Fshr	189	CAGGTCAACATACCGCTTGA	TCCCCAGGCTGAGTCATATC
Gata1	124	TTGTGAGGCCAGAGAGTGTG	CCGGTTCTGACCATTCATCT
Gata4	175	AAAACGGAAGCCCAAGAACC	ATAGTGAGATGACAGCCCGG
Gdnf	151	GACTTGGGTTTGGGCTATGA	AACATGCCTGGCCTACTTTG
Gfra1	152	AGACTTCGAGCAGGAGATGG	AGGTCTTTACGGATGTCAACG
Kitl/Scf	122	CGGGAATCCTGTGACTGATAA	GCCAACACCTGACTAGGAAA
Lhcgr	195	GCAGCTAATCTCGCTGGAGT	CTGGAGGGCAGAGTTTTCAG
Nrg1	172	AGGAACTCAGCCACAAACAAC	TCTTGAGGGGTTTGACAGGT
Pdpn	126	AATCTACTGGCAAGGCACCT	CAGTGGTTGTACTCTCGTGT
Sox9	141	GACTCCCCACATTCCTCCTC	CCCCTCTCGCTTCAGATCAA
Stra8	135	CTCCTCCTCCACTCTGTTGC	GCGGCAGAGACAATAGGAAG
Tuba1	171	ATTGGGGGAGGAGATGACTC	ATCCTCCTTGCCTGTGATGA
Usf1	150	GGAGGGCTCAACATAACGAA	AATCTCTGGCTTTGGACAGG
Usf2	152	GGAGGCGCGATTTGCTTATT	TTGTCCTCTGTGTGCCTGTC
Wnt4	144	ACTGGACTCCCTCCCTGTCT	TCACAGCCACACTTCTCCAG
Wnt5a	138	ATGCAGTACATTGGAGAAGGTG	CGTCTCTCGGCTGCCTATTT
Wnt6	152	GTGGACTTCGGGGATGAGAA	CCATGGCACTTACACTCGGT
Wt1	196	AGTTCCCAACCATTCCTTC	CATTCAAGCTGGGAGGTCAT

4.3.3   Targeted RNA sequencing (III)

Total RNA was isolated from snap-frozen adult mouse testes using the RNeasy Mini Kit (Qiagen, Hilden, Germany). Total RNA was treated with RNase-free DNase and purified using the RNAeasy MinElute Cleanup Kit (Qiagen, Hilden, Germany). A panel of target genes was selected for TruSeq Targeted RNA sequencing (Illumina, San Diego, CA, USA). These target genes consisted of testicular markers and cell-cycle-related and specific target genes expressed in juvenile and adult SCs (Table 2).

Table 2.   Target genes.

Name	Gene ID	Name	Gene ID	Name	Gene ID
Housekeeping					
Rpl19	19921	*Hprt*	15452	*Ppia*	268373
Paracrine control					
Inha	16322	*Inhba*	**16323**	*Inhbb*	16324
Sertoli cell					
Cldn3	2739	*Rhox5*	18617	*Gata1*	14460
Cldn11	18417	*TRalpha1*	21833	*Sox9*	20682
Wt1	22431	*Espin*	75526	*AMH*	11705
Ar	11835	*Gdnf*	14573		
Peritubular myoid cell					
Sma	11475	*calponin*	12797	*Myh11*	17880
Leydig cell					
3betaHSD	15497	*Cyp17a1*	13074	*Star*	20845
Spermatogonial stem cell					
Thy1	21838	*Lin28*	83557	*Plzf*	235320
Oct4/Pou5f1	18999	*Gfra1*	14585	*Oct2/Pou2f2*	18987
Spermatogonia					
Stra8	20899	*Kit*	16590	*AP2gamma/ Tfap2c*	21420
Meiotic cells					
Sycp1	20957	*Spo11*	26972		
Post-meiotic germ cell					
Piwil1	57749				
Cell cycle/Apoptosis					
E2F1	13555	*Rb1*	19645	*Apaf1*	11783
E2F2	242705	*Cdkn1b*	12576	*Fasl*	14103
E2F3a	NM_010093.3	*Cdkn2b*	12579	*Trp53*	22059
E2F3b	NM_001289920.1	*Ccne1*	25729	*Bax*	12028
E2F4	104394	*Ccne2*	12448	*Bcl-2*	12043

Name	Gene ID	Name	Gene ID	Name	Gene ID
E2F5	13559	**Ccnd1**	12443	**Bcl2l2**	12050
p107/Rbl1	19650	**Ccnd2**	12444	**Smad4**	17128
p130/Rbl2	19651	**Skp2**	27401		
		Putative E2F target genes			
Bmp2	12156		13361	**Jun**	16476
Fst	14313	**Tk1**	21877	**Cxcr4**	12767
Myc	17869	**Junb**	16477	**Smyd4**	319822
Differentially expressed genes in P10 SC-Rb-/- [8] _compared with ChIP-on-Chip_ [208,209]					
Tmem143	70209	**Col1a1**	12842	**Prcp**	72461
Mcm2	17216	**Epn1**	13854	**Scd2**	20250
Mif4gd	69674	**Fgd1**	14163	**Usp1**	230484
Adssl1	11565	**Mat2a**	232087	**Vamp2**	22318
Atf4	11911	**Mrps12**	24030		
Chek1	12649	**Pola2**	18969		
Differentially expressed genes in 1.5-month-old SC-Rb-/- [186] _compared with ChIP-on-Chip_ [208,209]					
Cdc6	23834	**Pold1**	18971	**Col4a2**	12826
Ccnb1	268697	**Rpa2**	19891	**Aplp1**	11803
Dnmt1	13433	**Rrm1**	20133	**Aurkb**	20877
H2afz	51788	**Rrm2**	20135	**Cx3cl1**	20312
Clspn	269582	**Timeless**	21853	**Icam1**	15894
Mcm5	17218	**Rbbp4**	19646	**Tgfbi**	21810
Mcm6	17219	**Rad51**	19361		
Pcna	18538	**Brca1**	12189		

4.4 Hormone assays (II–IV)

To measure serum FSH and LH, blood samples from adult male mice were extracted immediately after the mice were sacrificed. Serum was obtained by centrifugation, and samples were stored at −20°C until the hormone assays were performed. Hormone level quantification was performed using the FSH ELISA Kit (Novus Biologicals, Littleton, CO, USA), LH ELISA (Novus Biologicals; II), an immunofluorometric assay (III; DELFIA, Wallac, Turku, Finland) [210], or a Luminex 200 platform using a MILLIPLEX MAP Mouse Pituitary Magnetic Bead Panel (IV; Millipore, Burlington, MA, USA).

To measure the testosterone level in the testis or the FSH and LH content in the pituitary, tissue pieces were homogenized and total protein was measured. Testosterone level quantification was performed using a Pierce BCA kit (II; Thermo Fisher Scientific, Waltham, MA, USA) or a radioimmunoassay kit TESTO-CT2 (III;

Cisbio, International, France) [8] according to the manufacturer's protocol. Moreover, the FSH and LH content was detected with the Luminex 200 platform using the MILLIPLEX MAP Mouse Pituitary Magnetic Bead Panel (Millipore, Burlington, MA, USA). All the obtained concentrations were normalized to the weights of the tissues.

4.5 Fertility (III)

In each experimental group, male adult mice were bred with females of the same genetic background. All breeding couples were kept together for 24 h, or 48 h if no copulatory plugs were observed, and the number of pups and sex were recorded.

4.6 Sperm count (II)

Sperm were counted from the cauda epididymis of adult mice. All dissected cauda epididymides were slightly cut and placed in 1 mL of 1× phosphate-buffered saline (PBS) for 30 min. Samples were then pipetted up and down to homogenize the solution and to extract most of the sperm, and then 20 µL of each sample was counted in a Bürker chamber. Then, the number of sperm was calculated and normalized per 1 mL of solution.

4.7 Intracellular flow cytometry (I and III)

Rat testes were dissected under aseptic conditions and decapsulated in a Petri dish. Then, 10 mg of testicular tissue was placed in an Eppendorf tube containing 200 mL of an enzyme cocktail (1 mg/mL collagenase/dispase, 1 mg/mL hyaluronidase, and 1 mg/mL DNase I in Dulbecco's modified Eagle's medium/F12) on ice. Testicular tissues were then cut using McPherson-Vannas Scissors until small segments of 1 mm were observed. Then, 800 µL of the enzyme cocktail was added and samples were incubated for 30 min at 37℃. Every 5 min during incubation, samples were mechanically dissociated by pipetting up and down five times. After incubation, the solution was filtered through a 35 µm pore size filter and pelleted at 400 g for 10 min at 4℃. To differentiate only live cells in subsequent analyses, LIVE/DEAD (BD Falcon, BD Biosciences, NJ, USA) staining was performed. The stock stain was reconstituted in dimethyl sulfoxide and added to the sample at a final concentration of 1 : 10,000. The product of the LIVE/DEAD staining procedure was then incubated for 30 min on ice and pelleted as above.

Fixation was performed by adding 32% paraformaldehyde (PFA) to a final concentration of 4% PFA in the cell suspension under continuous vortexing. Then,

samples were incubated for 10 min at 37℃ under gentle rotation. To stop the reaction, the samples were placed on ice for at least 1 min and then pelleted by centrifugation as above. Permeabilization was performed first by dissolving the pellet in 100 µL of PBS and then adding 900 µL of cold 100% methanol under vortexing, followed by incubating the samples for 30 min on ice.

To detect intracellular antibodies, the same steps for common immunofluorescence were followed. First, samples were washed once with PBS, centrifuged at 1,200 rpm for 7 min at 4℃, resuspended in a blocking solution (0.5% normal serum), and incubated for 30 min at room temperature (RT). Primary antibodies (Table 3) were diluted in the blocking solution, added to the samples, and incubated for 1 h at RT. For antibodies that were not conjugated to fluorophores, fluorescence secondary antibodies were used. After primary and secondary antibody incubation, all cell suspensions were washed and resuspended in 0.2% bovine serum albumin (BSA) and 5 mg/mL RNase in PBS. DNA staining was performed with fxCycle or propidium iodide, and then the samples were analyzed using a Fortessa LSRII flow cytometer (Becton Dickinson, Franklin Lakes, NJ, USA).

4.8 Histology

Briefly, 4% PFA (I–IV) or Bouin's solution (II–IV)-fixed testes were embedded in blocks of paraffin. Then, 4–5 µm thick sections were cut and deparaffinized in xylene and ethanol series for staining.

For basic histological analysis, Bouin's fixed sections were stained with Mayer's hematoxylin, washed, and then counterstained with eosin solution (II, IV) or periodic acid–Schiff (III). Before mounting, the slides were dehydrated using an ascending gradient of ethanol and xylene.

4.8.1 Immunohistochemistry (III)

Briefly, 4% PFA-fixed testis sections were deparaffinized in xylene and descending ethanol series. After washing the slides in dH_2O, epitopes were exposed by cooking the slides in a pressure cooker in 0.1 M citrate buffer (pH 6.0). After cooling down, endogenous peroxidase was blocked by incubating the slides in 3% H_2O_2 for 10 min. After washing the slides with 1× Tris-buffered saline (TBS), the sections were incubated in normal serum for 1 h at RT to block unspecific bindings. Primary antibodies (Table 3) and biotinylated secondary antibodies were incubated for 1 h at RT between the washes. Signal detection was performed using 3,3′-diaminobenzidine chromogen, and counterstaining was performed using Mayer's hematoxylin. As a final step, the slides were dehydrated using an ascending gradient of ethanol and xylene and then mounted.

4.8.2   RNA *in situ* hybridization (III)

Briefly, 4% PFA-fixed testis sections were used to detect the mRNA of E2f3a and
E2F3ab using a 2-Plex Detection Kit (ACDBio, Newark, CA, USA). Custom and
control probes were designed by ACDBio. Vulcan Fast Red and black chromogen
were used to detect the mRNA signals from *E2f3a* and *E2f3ab*, respectively. All
procedures were performed according to the manufacturer's protocol with some
modifications. Mayer's hematoxylin was used as a counterstain. For
immunohistochemistry coupled to *in situ* hybridization, the slides were incubated in
5% horse serum in TBS to block unspecific bindings. Primary antibodies were
diluted in a blocking solution and incubated overnight at 4℃. Endogenous
peroxidase was blocked by incubating the slides in 3% H_2O_2. The signal was detected
using a biotinylated horse anti-rabbit antibody followed by Vector ABC-HRP
(Thermo Fisher Scientific, Waltham, MA, USA) staining. The slides were then air-
dried at RT and mounted with EcoMount and then imaged using a Pannoramic MIDI
FL slide scanner (Zeiss, Oberkochen, Germany).

4.8.3   Immunofluorescence

4.8.3.1   Immunofluorescence of paraffin-embedded fixed testes (I–IV)

In this study, PFA-fixed testis sections were labeled with specific markers to detect
the number of testicular cell populations, BTB, and cell cycle status of specific cells
(Table 3), as previously described [8]. Briefly, testis sections were deparaffinized in
xylene and descending ethanol series. After washing the slides in dH_2O, epitopes
were exposed by cooking the slides in a pressure cooker in 0.1 M citrate buffer (pH
6.0). After cooling down the slides, autofluorescence was blocked by incubating the
slides in 100 mM NH_4Cl for 10 min. Then, after washing the slides with TBS, the
sections were incubated in 5% normal donkey serum for 1 h at RT to block unspecific
bindings. Primary antibodies were diluted in a blocking solution (5% normal donkey
serum) and incubated overnight at 4℃. If the primary antibodies were not conjugated
to a fluorochrome, secondary antibodies conjugated to a fluorochrome were used.
After the incubation of the primary antibodies, the slides were washed in 0.05%
Tween 20 in TBS. Then, the secondary antibodies were diluted in a blocking solution
and incubated for 1 h at 37℃ in the dark. Notably, 4′,6-diamidino-2-phenylindole
(DAPI) was used as a counterstain at a concentration of 1 : 10,000 for 5 min. Finally,
the slides were mounted in a ProLong Diamond Antifade Mountant or
VECTASHIELD Mounting Medium (Vector Laboratories, Burlingame, CA, USA).
The sections were then imaged using an AxioImager M1 fluorescence microscope

(Zeiss) in the study I or a Pannoramic MIDI FL slide scanner (Zeiss) in the study II–IV.

4.8.3.2 Terminal deoxynucleotidyl transferase dUTP nick end labeling assay for paraffin-embedded fixed testes (III–IV)

Apoptotic cells were detected using the terminal deoxynucleotidyl transferase dUTP nick end labeling (TUNEL) assay as previously described [8]. Briefly, 4% PFA-fixed sections were deparaffinized and rehydrated. Then, antigen retrieval was performed in a pressure cooker in 0.1 M citrate buffer (pH 6.0). After cooling down the slides, autofluorescence was blocked by incubating the slides in 100 mM NH_4Cl for 10 min. After washing the slides with TBS, the positive control was incubated with grade I (3 U/mL) DNase I for 30 min at 37℃. Then, the reaction mixture, containing terminal deoxynucleotidyl transferase buffer, transferase, $CoCl_2$, and dUTP, was applied to the sections and incubated for 1 h at 37℃ in a humidified chamber. To stop the reaction, 300 mM NaCl and 30 mM sodium citrate in Milli-Q water were added and incubated for 15 min at RT. Then, after washing with PBS, the sections were incubated in 5% normal donkey serum for 30 min at RT. To reveal apoptotic cells, extrAvidin was applied to the sections for 30 min at 37℃, followed by washing the sections in PBS. Then, DAPI was used as a counterstain at a concentration of 1 : 10,000 for 5 min. Finally, the slides were mounted in a ProLong Diamond Antifade Mountant or VECTASHIELD Mounting Medium (Vector Laboratories). The sections were then imaged using an AxioImager M1 fluorescence microscope (Zeiss) in the study I or a Pannoramic MIDI FL slide scanner (Zeiss) in the study II–IV.

4.8.3.3 Immunofluorescence of testicular cryosections (II)

Dissected testes were fixed in 4% PFA overnight at RT, dehydrated in 20% sucrose solution in PBS, and embedded into an Optimal cutting temperature (OCT) compound. Notably, 10 µm thick sections were used for staining (Table 3). Briefly, testis sections were deparaffinized in xylene and descending ethanol series. After washing the slides in dH_2O, epitopes were exposed by cooking the slides in a microwave oven in 0.1 M citrate buffer (pH 6.0) for 15–20 min. Then, after washing the slides with PBS, the sections were incubated in 5% normal donkey serum and 5% BSA in 0.2% Tween 20 in PBS (PBST) for 1 h at RT to block unspecific bindings. Primary antibodies were diluted in 1% BSA in 0.2% PBST and incubated overnight at 4℃. After the incubation of the primary antibodies, the slides were washed in 0.1% PBST. Then, the secondary antibodies were diluted in 1% BSA in

0.2% PBST and incubated for 1 h at 37℃ in the dark. The slides were then mounted in a VECTASHIELD Mounting Medium containing DAPI (Vector Laboratories), and the sections were imaged using a Zeiss AxioImager microscope.

4.8.3.4   Immunofluorescence of whole mounts (II)

Testes were dissected under aseptic conditions and decapsulated in a Petri dish containing cold PBS. Then, the seminiferous tubules were separated carefully and then pipetted up and down with a 1 mL with a cut tip several times. The seminiferous tubules were transferred to Falcon tubes, which were inverted several times and left to sediment on ice. After two washes in PBS, the seminiferous tubules were fixed in 4% PFA on a rotating table for 4–6 h at 4℃. The samples were left to sediment on ice and then washed three times in PBS for 10 min at 4℃, followed by storage at 4℃ until staining.

For immunolabeling, whole mounts were blocked with 2% BSA and 10% FBS in 0.3% Triton X-100 in PBS (PBSX) on a rotating table for 1 h at RT. Primary antibodies (Table 3) were diluted in 1% BSA in 0.3% PBSX and incubated overnight at 4℃. After washing with PBSX, secondary antibodies were prepared in 1% BSA in 0.3% PBSX and incubated for 2 h at RT in the dark. Notably, DAPI was used as a counterstain before mounting the tubules with VECTASHIELD Mounting Medium, and common nail polish was used to seal the coverslip.

4.8.3.5   Whole-mount staining and imaging of the vibratome-sectioned testis (IV)

To show the expression of PLVAP in the testicular blood vessels, we performed immunofluorescence staining on vibratome-sectioned testes. Briefly, dissected testes were fixed in 2% PFA on ice for 1 h followed by dehydration in an increasing methanol series. The samples were dehydrated and kept in 100% methanol at −20℃ overnight. On the next day, rehydration was performed in a decreasing methanol series and samples were embedded in 4% low-melting-point agarose. Then, 200 μm sections were cut using a VT1200 S vibratome (Leica, Wetzlar, Germany). The sections were detached from agarose, blocked with 1% BSA and 0.4% PBSX at RT for 1 h, and incubated with a primary antibody at 4℃ overnight. After washing, the samples were incubated with a secondary antibody at RT for 2 h, and then the sections were stained with Hoechst and rinsed with 0.4% Triton X-100. The samples were then mounted on glass-bottom well dishes with ProLong Gold without DAPI (Thermo Fisher Scientific, Waltham, MA, USA). Then, the sections were imaged using a spinning disk confocal microscope (Intelligent Imaging Innovations, Göttingen, Germany) equipped with an ORCA-Flash4.0 V2 sCMOS camera

(Hamamatsu, Shizuoka, Japan) and C-Apochromat 40x/1.1 objective and using SlideBook 6 software (Intelligent Imaging Innovations).

Table 3. Antibodies used in the study.

Target	Host	Cat. #	Manufacturer	Application	Dilution	Study
Vimentin	rabbit	9854	Cell signaling	FC, IHC, IF	1/50	I, III
γH2A2-Ser139	mouse	05-636	EMD Millipore	FC	1/100	I
Ki67	rat	11-5698-82	eBioscience	IHC, IF	1:200-1:400	III, IV
	rat	14-5698-82	Thermo Fischer	IF	1:100-1:400	II
p130	rabbit	sc-317	Santa Cruz	IHC	1/800	III
p107	rabbit	sc-318	Santa Cruz	IHC	1/1600	III
E2F3a	mouse	MS-1063-P0	Thermo Fischer	IHC	1/200	III
E2F3	rabbit	sc-878	Santa Cruz	IHC	1/1600	III
AR	rabbit	sc-816	Santa Cruz	IF	1/200	III
AR	rabbit	ab133273	Abcam	IF	1:100-1:400	II
ESPIN	mouse	611656	BD Biosciences	IF	1/400	II, III, IV
SOX9	rabbit	ab5535	EMD Millipore	IF	1/400	II, III, IV
	mouse	53-9765-82	Thermo Fischer	IF	1:100	II
CLDN11	rabbit	sc-25711	Santa Cruz	IF	1:100-1:400	II, III, IV
Gata1	rat	sc-265	Santa Cruz	IF	1:100-1:400	II
Gata4	goat	sc-1237	Santa Cruz	IF	1:200	II
WT1	goat	sc-15421	Santa Cruz	IF	1:100-1:400	II
PLZF	rabbit	sc-22839	Santa Cruz	IF	1:100-1:400	II, IV
USF1	rabbit	sc-8983	Santa Cruz	IF	1:100-1:400	II
GFRα1	goat	AF560	R&D Systems	IF	1:400	II
DNMT3	mouse	IMG-268A	Novus Biologicals	IF	1:100	II
3βHSD	rabbit	KO607	Trans Genic	IF	1:200	IV
CYP11A1	goat	sc-18043	Santa Cruz	IF	1:200	IV
SMA	mouse	ab184675	Abcam	IF	1:100	IV
PNA		RL-1072	Vector Laboratories	IF	1:1000	IV
Scp3	mouse	ab97672	Abcam	IF	1:200	IV
CD31	rat	102510	BioLegend	FC, IF	1:100	IV
MECA	rat	MECA32-17-8 AK 2028/01	InVivo	IF	1:100	IV

4.9 Human chorionic gonadotropin replacement (IV)

Due to the lack of gonadotropin stimulation, one-week old mice were treated with 1 UI of human chorionic gonadotropin (hCG, Pregnyl; MSD, Oss, The Netherlands) for three weeks. Injections were performed three times a week intraperitoneally. Mice were sacrificed at the age of five weeks. Serum samples, testes, and epididymides were collected for analysis.

4.10 Statistical analysis of the data (I–IV)

All values are presented as mean ± standard error of the mean. All statistical analyses were performed using GraphPad Prism 5 software version 6 (GraphPad Software, San Diego, CA, USA). The unpaired t-test was used for data with two experimental groups (II, IV), and one-way analysis of variance (ANOVA) was used for data with three or more experimental groups, followed by Tukey's test (III). For statistical analysis of TruSeq Targeted RNA sequencing, the negative binomial distribution model was used. P-values were provided by the TruSeq Targeted RNA sequencing application v1.0. P-values less than 0.05 were considered as a threshold for statistical significance.

5 Results and Discussion

The following are the main results of studies I–IV:

I. Intracellular flow cytometry is a newly developed, fast, accurate tool for quantifying rodent testicular cell populations.

II. USF1 is a transcription factor involved in the regulation of the balance between self-renewal and differentiation of SSCs.

III. E2F3 is not essential for adult SC function. However, the interaction between pRb and transcription factor E2F3 is involved in the regulation of the maintenance of adult SCs in a quiescent state and, therefore, determines their function in adult testes.

IV. PLVAP indirectly regulates the endocrine function of the testis for its development and adult function.

5.1 A rapid intracellular flow cytometry protocol to study rodent testicular dynamics (I)

Various morphometric methods, such as manual quantification, of stained tissues or cells have been conventionally used in routine laboratory analyses. When studying the testis, immunohistochemistry and immunofluorescence staining are considered helpful in the identification of specific cell types. However, using morphometric techniques in a heterogeneous organ like the testis is laborious and time-consuming. Thus, using flow cytometry technology to study testicular populations coupled to DNA staining and/or specific antibodies has improved the screening of testicular cell composition [137–140]. Unlike previously reported protocols, we proposed a flow-cytometry-based protocol that allows quick assessment of rodent testis phenotype in one working day.

5.1.1 Protocol development and optimization

The principal goal of this study is to develop an accurate and fast flow-cytometry-based method for the analysis of testicular cell populations. As we wanted to obtain

information on different types of cell populations, signaling cascades, and molecular pathways, we opted to develop a protocol suitable for fluorescent intracellular antibody detection. While developing our method, we used rat testis ontogenesis as a model (5, 10, 16, and 24 days old and adult rats) as the testicular composition and maturation at different time points are well characterized [211,212].

Testicular single-cell suspensions are prepared in four steps: mincing of the tissue, enzymatic/mechanical dissociation, fixation, and permeabilization (I; Figure 1). The enzymatic and mechanical step was optimized step by step to obtain representative testicular cell population ratios (I; Figure 1) that mimic the natural cell dynamics during rodent testicular development. To avoid the destruction of fragile pachytene spermatocytes, the maximum number of mechanical pipetting steps during enzymatic incubation was set to five. Fixation and permeabilization of the cell suspension are considered critical steps to use intracellular antibodies, for which we used 4% PFA and cold methanol, respectively. This protocol enables the storage of testicular single-cell suspensions for long periods of time at −20℃. If needed, these suspensions can also be delivered to other laboratories for further staining and analysis.

To distinguish the heterogeneous cell populations in our single-cell suspension, we used propidium iodide or fxCycle as a DNA stain. Flow cytometry analysis showed that we recovered representative amounts of testicular cell populations. In rats that are 5–16 days old, the testicular cell suspension was found to consist of 2C cells in the S-phase of the cell cycle and 4C populations. Notably, the ratio of 2C (SCs, spermatogonia) to 4C (primary spermatocytes) populations was found to change when 1C (spermatids) cells were observed in the testes of 24-day-old rats. By the time the animal reaches adulthood, the 1C population becomes predominant in comparison to the 2C and 4C populations (I; Figure 3). According to these results, the cell number rates in different cell populations obtained by our optimized protocol were found to be similar to those in previous morphometric studies [211,216].

5.1.2   Intracellular antibody staining

To confirm the presence of representative populations and to gather more information about the somatic/germ cell dynamics, we optimized the fluorescence intracellular staining technique to the obtained single-cell suspension. We used vimentin antibody (expressed in SCs and Leydig cells) to monitor the somatic cells of the testis and phosphorylated γH2AX antibody to detect germ cells. After intracellular antibody staining, the single-cell suspension was counterstained with a DNA stain and analyzed using flow cytometry.

The expression of vimentin was found to mimic the proliferation dynamics of somatic cells during rat testicular development [211,213] (I; Figure 4). Before

spermatogenesis, the composition of the rat testis consisted mostly of SCs and spermatogonia. As expected, the rat testicular cell population at the ages of 5 and 10 days was found to consist mostly of vimentin-positive cells. At the age of 16 days, the proportion of vimentin-positive cells starts to decrease as the proliferation of SCs gradually ceases to form the BTB, and spermatogonia begin to proliferate. From the age of 24 days, when the first haploid cells emerge, to the adult age, the relative abundance of vimentin-positive cells decreases as the seminiferous tubules consist mostly of germ cells at different differentiation steps (I; Figure 4). This protocol is considered to be helpful in recovering a representative amount of somatic cells of young and adult testes.

In the testis, phosphorylated γH2AX histone protein is associated with both DNA double-stranded breaks and sex vesicle formation. This protein is expressed in germ cells from differentiated spermatogonia (2C) to pachytene spermatocytes (4C) and in steps 11 to 14 in RSs (1C) [214,215]. From our results, at the age of 16 days, most of the testicular cells were negative for γH2AX, because somatic cells were undergoing proliferation, and undifferentiated spermatogonia were present (I; Figure 5). As expected, most of the 4C populations were positive for γH2AX staining in the adult testis (I; Figure 5). These results prove that this antibody can be useful in the detection of specific subsets of germ cells in rodents.

Despite the broad availability of antibodies on the market, validation of immunofluorescence staining for flow cytometry analysis is challenging because many antibodies do not share the same staining protocols. Our aim was to use multiple antibodies at once; however, some of the antibodies (PLZF, SOX9, SMA, KI67, and protamine 2) did not perform as expected. This phenomenon may be related to the fixation and permeabilization steps that alter the target epitopes. Additionally, interspecies differences may have limited the performance of these antibodies, restricting the availability and use of suitable antibodies among rodents.

Despite the advantages of our method and the large number of cells that can be analyzed using a flow cytometer, this method cannot replace the golden-standard histological analysis. However, our approach can provide much more targeted information to understand and complement histological data.

5.1.3 Application of the flow-cytometry-based method

Since the publication of the flow-cytometry-based method, it has been adapted to be used with different amounts of rat and mouse testicular tissues (Table 4).

Table 4. Application of the flow cytometry protocol in additional projects.

Studies	Specie	Analyzed tissue	Staining
Eggert A., <u>Cisneros-Montalvo S</u>., Anandan S., Musilli S., Stukenborg J.B., Adamsson A., Nurmio M., Toppari J. 2019. The effects of PFOA (Perfluorooctanoic acid) on fetal and adult rat testis. Reprod Toxicol. 11;90:68-76.	Mouse	20 pieces of 2 mm seminiferous tubules were pooled per sample	Vimentin and DNA staining
Hakkarainen, J., Zhang F.P., Jokela H., Mayerhofer A., Behr R., <u>Cisneros-Montalvo S</u>., Nurmio M., Toppari J., Ohlsson C., Kotaja N., Sipila P., and Poutanen M. 2018. Hydroxysteroid (17beta) dehydrogenase 1 expressed by Sertoli cells contributes to steroid synthesis and is required for male fertility. Faseb J. 32:3229-3241.	Mouse	10mg of testis tissue per sample	DNA staining
Reda, A., Albalushi H., <u>Montalvo S.C.</u>, Nurmio M., Sahin Z., Hou M., Geijsen N., Toppari J., Soder O., and Stukenborg J.B. 2017. Knock-Out Serum Replacement and Melatonin Effects on Germ Cell Differentiation in Murine Testicular Explant Cultures. Ann.Biomed.Eng. 45:1783-1794.	Mouse	3-5 mg of testis tissue per sample	DNA staining
Rotgers, E., Nurmio M., Pietilä E., <u>Cisneros-Montalvo S.</u>, and Toppari J. 2015. E2F1 controls germ cell apoptosis during the first wave of spermatogenesis. Andrology. 3:1000-1014.	Mouse	10mg of testis tissue per sample	DNA staining

5.1.4 Update and future perspectives (I)

Notably, after we published our protocol, we succeeded in downscaling it, allowing us to analyze only a few milligrams of testis tissues [217] and even pieces of the seminiferous tubules [218] (Table 4.). Our protocol can be used for quick screening of testicular phenotypes of transgenic animals and testicular effects of *in vivo* drug exposure, and it can also be used to study the cell dynamics of *in vitro* cultures of seminiferous tubule pieces. Recently, we have added the phospho-histone H3 (Ser10) antibody to our antibody panel to analyze mitotic and meiotic progression during testicular development.

In the future, further optimization of a larger panel of specific antibodies would provide additional information on somatic and germ cell dynamics and signaling pathways during testicular development and spermatogenesis, which would have significant potential in several clinical applications, such as the characterization, diagnosis, and monitoring of disorders of human male reproduction.

5.2 USF1 is required for the maintenance of spermatogonial stem cells (II)

USF1 is a ubiquitously expressed transcription factor that has been reported to participate in biological processes from lipid to glucose metabolism pathways. Despite its reported expression in only the supporting cells of the testis, no essential function has been found for USF1 in male fertility. In this study, we demonstrated that USF1 is also expressed in SSCs and plays a crucial role in male fertility.

5.2.1 Testicular phenotype of *Usf1*$^{-/-}$ (II)

It was observed that the loss of USF1 produces a significant decrease in body and testis weight in mice aged 1 to 20 weeks (II; Figures 2A–2C). In addition, a significant difference was observed in the relative testis weight (testis weight/body weight) in 1, 12, and 20-week-old mice with Usf1$^{-/-}$ testes (II; Figure 2D). At the age of 1–8 weeks, histological analysis of the Usf1$^{-/-}$ testis showed a normal seminiferous tubule architecture; however, the testis atrophied gradually by 12 weeks of age (II; Figure 2E). At this time point, some seminiferous tubules display complete spermatogenesis, while others consist of fewer spermatogenic layers or an SC-only phenotype. To evaluate the spermatogenic defect level in Usf1$^{-/-}$, we quantified the number of tubule cross sections with empty tubules or those lacking one to three spermatogenic cell layers at different time points. As a result, Usf1$^{-/-}$ testes showed a larger number of tubule cross sections missing one to three spermatogenic cell layers and empty tubule cross sections from eight weeks old onwards (II; Figures 2K–2N) in comparison to the control animals. Notably Usf1$^{-/-}$ mice were initially fertile with sperm counts similar to those of the controls at the age of eight weeks; however, similar to the histological findings, the sperm count in 12-week-old mice was found to be significantly lower than in the controls (II; Supplementary Figure 3C). Serum FSH and LH were found to be significantly high in Usf1$^{-/-}$ mice, which is a sign of failure of the testes. Notably, the level of ITT, but not that of serum testosterone, was also found to be significantly higher in Usf1$^{-/-}$ mice than in the control animals (II; Figures 3A–3D). According to these data, the testes of Usf1$^{-/-}$ mice show age-related degeneration of the seminiferous epithelium, resulting in a decrease in sperm production. Besides, the testicular phenotype appears not be caused by insufficient gonadotropin stimulation or lack of androgen stimulation.

5.2.2   Somatic cell status in *Usf1⁻/⁻* (II)

To evaluate the protein expression of USF1 in a control testis, we performed indirect immunofluorescence in PFA-fixed sections. Notably, a strong signal was detected in SCs and a weak signal was detected in interstitial cells (II; Figure 1C). To evaluate the possible dysfunctional status of somatic cells, immunofluorescence staining was performed with specific markers, in addition to further quantification of positive cells. SOX9 and 3β-HSD antibodies were used as specific markers for SCs and Leydig cells, respectively. KI67 antibody, a proliferation marker, was also added to the assay to provide information regarding the proliferation status of somatic cells in the $Usf1^{-/-}$ testes at different time points. Quantification revealed that the number of SCs (SOX9-positive) and Leydig cells (3β-HSD-positive) in proliferation per cross section in the $Usf1^{-/-}$ testes is similar to that of the control mice at 4, 8, and 12 weeks of age (II; Supplementary Figure 4A, Figures 3E and 3F). The normal relative amount of Leydig cells in the $Usf1^{-/-}$ does not explain the high ITT levels. However, it may be partially explained by the higher ratio of Leydig cells to the other cell types present in the degenerating testis. Furthermore, AR, which is essential for lifelong fertility, showed a similar mRNA and protein expression in both the $Usf1^{-/-}$ and control testes (II; Figure 3H). Also, immunofluorescence of ESPIN and CLAUDIN 11, which are components of the BTB that also reflect the terminal differentiation of SCs, did not show any differences between the control and $Usf1^{-/-}$ testes (II; Supplementary Figures 4F and 4G). Collectively, these data suggest that the Sertoli and Leydig cell cycle dynamics are not altered in $Usf1^{-/-}$ testes.

As it has been reported in previous studies that USF1 and USF2 have compensatory functions in the absence of one of them [159,224], the unaltered Leydig cell and SC development in $Usf1^{-/-}$ mice may be due to USF2 compensation in the absence of USF1. Therefore, Sertoli/Leydig cell-specific knockout models would be beneficial to evaluate the extent of compensation and the effect of *Usf1* deletion at a transcriptomic level.

5.2.3   USF1 is expressed in spermatogonial stem cells in the testis

As low-level protein expression is difficult to detect by immunofluorescence in standard PFA-fixed testis sections, indirect immunofluorescence staining of USF1, SOX9, PLZF (expressed in undifferentiated, progenitor, and early differentiating spermatogonia), and DNMT3 (expressed in A1–A4, In, B, and preleptotene spermatocytes) antibodies was performed in fixed whole-mount samples. Notably, USF1 protein expression was detected, as previously shown, in SCs (SOX9 and USF1 double-positive cells) and also in spermatogonia (PLZF and USF1 double-

positive cells), and a higher signal of USF1 was detected from PLZF-positive, DNMT3A-negative cells. Further characterization using immunofluorescence revealed that USF1-positive undifferentiating spermatogonia also express GFRα1, a marker of A_s and A_{pr} SSCs (II; Supplementary Figure 1A; Figures 1D and 1E).

5.2.4 USF1 regulates the self-renewal of spermatogonial stem cells (II)

As USF1 protein expression was detected in spermatogonia, we evaluated whether the population of spermatogonia is affected in $Usf1^{-/-}$ testes using indirect immunofluorescence with PLZF antibody. Quantification of PLZF-positive cells in the $Usf1^{-/-}$ testes showed significant depletion of this population from the age of eight weeks onwards (II; Figure 5B).

As apoptosis and overproliferation are the principal causes of germline stem cell depletion, we evaluated these alternatives using immunofluorescence in fixed whole-mount seminiferous tubules. Notably, cleaved caspase-3 staining did not show increased apoptosis within GFRα1-positive cells (a marker of A_s and A_{pr} spermatogonia) in $Usf1^{-/-}$ adult testes (II; Supplementary Figure 8). However, when the proliferation rate within the GFRα1-positive cells was quantified, clear differences were observed in the seminiferous tubules of the $Usf1^{-/-}$ mice. A significantly large number of proliferating A_s undifferentiated spermatogonia were observed in the seminiferous tubules of $Usf1^{-/-}$ mice. Furthermore, a large, but insignificant, number of proliferating A_{pr} undifferentiated spermatogonia were observed in the seminiferous tubules of $Usf1^{-/-}$ mice (II; Figures 6A–6D). These results suggest that the failure of spermatogenesis observed may be attributed to the continuous proliferation of A_s and, as a consequence, the gradual exhaustion of the SSC pool.

In normal spermatogenesis, a subpopulation of SSCs exit the cell cycle and a subset of them delineate into a differentiation-primed state to give rise to more differentiated germ cells. In the case of $Usf1^{-/-}$, A_s spermatogonia do not exit the cell cycle, causing gradual exhaustion of the SSC pool at the adult stage. This may explain why $Usf1^{-/-}$ testes at a young age display normal-looking spermatogenesis but fail to maintain spermatogenesis with age. This type of failure has also been reported in other mouse models, including mice deficient in $Plzf$ [35,36], $Ta4b$ [37], and Erm [219], which are fertile at a young age but then their seminiferous tubules start to gradually lose their capacity to maintain steady spermatogenesis.

5.2.5   Gene expression analysis

We evaluated the mRNA levels from whole testes of important paracrine factors (*Cxcl12*, *Csf1*, *Fgf2*, *Nrg1*, *Wnt4*, *Wnt5a*, *Wnt6*, and *Bmp4*) that determine the mouse testis stem cell niche integrity. However, no significant differences were found at any of the time points evaluated in comparison to the controls (II; Supplementary Figures 6 and 7). As *Gdnf* and *Scf* are very important for the differentiation of spermatogonia, we evaluated the mRNA expression of them also in isolated stage-specific seminiferous tubules from $Usf1^{-/-}$ and control testes. We observed a significantly increased level of *Gdnf* at stages II–V as well as an increased level of *Scf* at stages VII and VIII in comparison to the controls (II; Figures 5C and 5D). As *Gdnf* is related to the mitotic status of undifferentiated spermatogonia and its levels are low in these stages in WT testes [220–222], we hypothesized that *Gdnf* contributes to the continuous proliferation of A_s spermatogonia in $Usf1^{-/-}$ testes. Besides, as *Gdnf* is regulated by FSH [223], the high levels of FSH observed in the plasma of $Usf1^{-/-}$ mice may contribute to the elevated levels of *Gdnf* in the testis. Collectively, these results suggest that the paracrine milieu of the SSC niche in $Usf1^{-/-}$ testes is similar to the one in the controls. However, the overexpression of *Gdnf* may contribute to the continuous proliferation of A_s spermatogonia in $Usf1^{-/-}$ testes.

5.2.6   Future perspective (II)

Previously, the USF1 transcription factor has been reported to be expressed only in the supporting cells of the testis, the SCs. However, in our study, indirect immunofluorescence of USF1 in whole fixed seminiferous tubules revealed that USF1 is also expressed in SSCs and undifferentiated spermatogonia. This expression pattern resembles that of PLZF, a routinely used marker for undifferentiated spermatogonia. Thus, USF1 is regarded as a potential marker of undifferentiated spermatogonia.

During our study, we made use of a global *Usf1* knockout model, which makes difficult the interpretation of direct cell-specific or indirect effects from other cells or organs. Despite the fact that, not alteration was observed in the proliferation and maturation of the somatic cells in the $Usf1^{-/-}$, it can not be discarded the possibility of a gradual failure in function after their maturation. In such a situation, somatic/germ cell specific knockout models would be beneficial to evaluate the effect of the absence of *Usf1* in specific cell types. The molecular mechanism by which the deficiency of *Usf1* causes continuous proliferation of undifferentiated spermatogonia has not been addressed in this study. Therefore, further research is needed on this subject as the control of self-renewal and differentiation of stem cells may have a potential future clinical application in cancer stem cell treatment.

Mice with inactivated USF1 gene show improved lipid profile. Therefore, it has been reported that USF1 is a potential target for diabetes, obesity, and other cardiometabolic diseases [6]. In our study, we showed that complete deletion of USF1 is not useful for male fertility in the long run. However, haploinsufficiency of *Usf1* would be a good option as a therapeutic target because heterozygous mice also exhibit good lipid profiles with no alteration in testicular development and function [6].

5.3 RB/E2F3 is required for the terminal differentiation of Sertoli cells (III)

We have previously reported the role of RB in the maintenance of adult mouse SCs in a quiescent stage. We also showed that RB interacts with E2F3 to maintain adult SCs in a quiescent state and that shRNA-mediated knockdown of E2f3 partially recovers the phenotype [8]. In this study, we revealed the dispensable function and expression pattern of E2F3 during SC development. In addition, through SC-specific deletion of *Rb* and *E2f3* simultaneously, we obtained complete recovery of the phenotype and further unraveled the RB/E2F3 interaction in the adult SCs.

5.3.1 E2F3 expression in mouse testis (III)

To study the expression of both E2F3 isoforms in SCs, we performed immunohistochemistry staining of E2F3a and E2F3ab antibodies at the age of 6, 10, 20, and 40 days in control testes. It was found that the E2F3a protein is expressed in a subpopulation of SCs in the testes of six-day-old mice. Notably, the number of SCs positive for E2F3a increased with age until the age of 20 days when all SCs were positive for E2F3a (III, Figure 1A). To evaluate whether the expression of the E2F3a isoform is associated with the engagement of SC differentiation, we performed immunohistochemistry of KI67 together with the E2F3a antibody. However, no correlation was observed in the KI67 and E2F3a staining, as both double E2F3a-positive/KI67-positive and E2F3a-positive/KI67-negative SCs were detected (III, Figure 1A). It was also observed that the expression pattern of E2F3ab is similar to that of E2F3a in SCs. However, in the testes of mice aged 6 and 10 days, E2F3ab was also found to be expressed in spermatogonia (III, Figure 1B). Collectively, these data show that both E2F3 isoforms are expressed with different patterns: the expression of E2F3a is gradual in SCs but not linked to the cell cycle exit of SCs [8,225] and the expression of the E2F3b isoform is exclusive in the spermatogonia of young testes.

5.3.2 E2F3 is not required for mouse testicular development and function (III)

To evaluate the role of *E2f3* in mouse SCs, a mouse model in which the expression of *E2f3* is absent from SCs (SC-*E2f3*−/−) was studied. Despite the loss of *E2f3*, these SC-*E2f3*−/− mice did not face any problems during development. Their relative testis weight (testis weight/body weight) did not show a significant difference at the age of two months (III; Supplementary Figure 1A) in comparison to the controls. At the age of five months, their relative testis weight became significantly smaller; however, they sired healthy pups and no significant differences were observed in the number of pups per litter as compared with the control males (III; Table 1). Histologic analysis of the SC-*E2f3*−/− testis did not show any alteration in the seminiferous architecture at either age (III; Supplementary Figure 1C).

To evaluate whether this small relative testis size was due to increased apoptosis in the SC-*E2f3*−/− testes, TUNEL staining was performed. However, the SC-*E2f3*−/− testes were found to have an apoptotic index similar to that of the control mice (III; Supplementary Figure 1E). Furthermore, flow cytometry analysis confirmed that the number of testicular cell populations according to their DNA content in the SC-*E2f3*−/− testes was similar to that of the control mice (III; Supplementary Figure 1D). Collectively, these data indicate that *E2f3* is redundant in SCs. Notably, SC-*E2f3*−/− mice showed normal testicular development and fertility compared to those of the control mice. As a compensatory function has been reported among the E2F transcription factors [226], we proposed that the status of SCs was not compromised in SC-*E2f3*−/− most probably by a compensatory effect by other E2F transcription factors.

5.3.3 The testicular phenotype of the SC-Rb−/−E2f3+/+, SC-Rb−/−E2f3+/− and SC-Rb−/−E2f3−/− mice (III)

We obtained an SC-*Rb*−/−*E2f3*+/+ and SC-*Rb*−/−*E2f3*−/− mouse lines in which the SCs lack *Rb* or *Rb* and *E2f3* expression, respectively. Despite having a different genetic background, this mouse line had a phenotype similar to the one described before, in which SC-*Rb*−/− mice display impaired testicular function due to adult SC dysfunction [8,186]. We previously showed that knocking down *E2f3* with shRNA in the absence of *Rb* partially restores the seminiferous tubule architecture of SC-*Rb*−/−. Thus, to investigate whether double knockdown of *Rb* and *E2f3* in SCs would fully restore the infertility phenotype, we studied the SC-*Rb*−/−*E2f3*+/+ mouse line.

As expected from previous studies [8], the relative testis weight (testis weight/body weight) of SC-*Rb*−/−*E2f3*+/+ mice was found to be significantly lower than that of the control mice. Moreover, the relative testis weights of *E2f3*-haploinsufficiency (SC-*Rb*−/−*E2f3*+/−) and *E2f3*-KO (SC-*Rb*−/−*E2f3*−/−) mice were found to be

comparable to those of the control mice (III; Figure 2A). Fertility test showed that male SC-*Rb*−/−*E2f3*+/+ mice were infertile as only immature germ cells were detected in the cauda epididymis, and they were not able to sire pups (III; Figure 5A, Table 1). On the contrary, the cauda epididymis of SC-*Rb*−/−*E2f3*+/− and SC-*Rb*−/−*E2f3*−/− mice showed mature sperm, and they were able to sire pups, though not comparable to the controls (III; Figure 5A, Table 1). Histological analysis of testis reflected the epididymal and fertility test findings. The seminiferous tubule architecture of the SC-*Rb*−/−*E2f3*+/+ testis was found to be atrophied at the age of 2.5 months. Empty seminiferous tubules or seminiferous epithelia with few cells or layers were abundant. Notably, the phenotype of *E2f3*-haploinsufficiency (SC-*Rb*−/−*E2f3*+/−) mice was found to be partially recovered as most tubules exhibited full spermatogenesis; however, few tubules still exhibited altered spermatogenesis. However, the double knockdown of *Rb* and *E2f3* in SCs fully restored the infertility phenotype of the SC-*Rb*−/−*E2f3*+/+. Similar to the controls, the seminiferous tubules displayed complete spermatogenesis.

These data indicate that the deletion of both alleles of *E2f3* in the absence of *Rb* was able to fully recover the phenotype as they consisted of seminiferous tubules with full spermatogenesis similar to the control mice (III; Figure 2B).

5.3.4   E2F3 induces cell cycle reentry in adult Sertoli cells in the absence of retinoblastoma protein (III)

According to our previous study, adult SCs in SC-*Rb*−/− reenter the cell cycle and cannot support spermatogenesis [8]. To evaluate whether the double deletion of *Rb* and *E2f3* restores the status of adult SCs, indirect immunofluorescence of SOX9 (a marker of SCs) and KI67 was performed at the age of 2.5 months.

It was found that the SC-*Rb*−/−*E2f3*+/+ testis had a significantly higher rate of adult SCs in proliferation than the control mice. One *E2f3* allele was able to induce SC proliferation in the adult testis in the absence of Rb (SC-*Rb*−/−*E2f3*+/−). Nevertheless, the deletion of both *E2f3* copies was able to block ectopic proliferation, as the proliferation rate decreased to the same level as in the testis of the control animals (III; Figures 3A and 3B). This recovery system has also been reported in a *Drosophila* model by Greenspan et al. [227]. The lack of Rbf (*Drosophila* homolog of RB) in the hub cells of the testis was found to induce cell cycle reentry and the formation of ectopic stem cell niches. Moreover, the phenotype was rescued by the knockdown of E2F. Besides, *E2f3* deletion was also found to rescue the proliferation defect in lens and cells from the central nervous system [228] and pituitary tumors [229] lacking *Rb*. Our results and reported data indicate a conserved role of RB-E2F in the control of a quiescent status. To evaluate the terminal differentiation status of adult SCs, we performed immunofluorescence staining of CLAUDIN 11

and ESPIN, which are components of the tight junctions and ectoplasmic specializations of the BTB. The results showed that the BTB of the SC-*Rb*−/−*E2f3*+/+ testis was disrupted. In line with the observation described above, SC-*Rb*−/−*E2f3*−/− mice were found to have a normal BTB and ectoplasmic specialization (III; Figure 5B). To evaluate whether the active proliferation of SCs in SC-*Rb*−/−*E2f3*+/+ was related to cell transdifferentiation, FOXL2 immunofluorescence staining was performed as granulosa cells in the ovary are positive for this protein. However, the adult SCs in SC-*Rb*−/−*E2f3*+/+ did not yield any FOXL2-positive signal (III; Supplementary Figure 2).

Collectively, these data indicate that the double deletion of *Rb* and *E2f3* was able to restore the quiescent status of adult SCs and also the abnormal BTB seen in the SC-*Rb*−/−*E2f3*+/+ testis. As RB and E2F3 physically interact in SCs [8], RB/E2F3 may be associated with SC differentiation to an adult phenotype. Moreover, RB is probably recruited by E2F3a to silence genes related to proliferation or induce gene transcription associated with maturation.

5.3.5   Gene expression analysis (III)

The mRNA expression levels of the selected proteins were measured from whole testes at the age of 2.5 months. In the *Rb*−/− fetal testis, p27 (CDK inhibitor 1B) compensates the lack of *Rb* and SKP2 (S-phase kinase-associated protein 2) inhibits p27 by proteasomal degradation [184]; therefore, we evaluated whether this compensation also occurs in our mouse lines. However, no significant changes in the expression level of *p27* between the experimental groups and the control mice were observed. However, the expression level of *Skp2* was found to be significantly downregulated in the SC-*Rb*−/−*E2f3*+/+ testes, and expression was restored in SC-*Rb*−/−*E2f3*−/−, suggesting that this compensatory mechanism also operates in the adult testis (III; Figures 3C and 3D).

Despite the active proliferation of adult SCs in the SC-*Rb*−/−*E2f3*+/+ testes, they seemed to maintain a transcriptional program similar to that of mature SCs, as the expression levels of *Wt1*, *Sox9*, *Gata1*, and *Gdnf* remained unaffected (III; Figure 3E). Moreover, as no SC tumors were visible, we also evaluated the pro- and antiapoptotic *Trp53* and *Bcl-2* expression levels. It was observed that the expression level of *Trp53* did not change in the SC-*Rb*−/−*E2f3*+/+ testes, but it significantly decreased in the SC-*Rb*−/−*E2f3*−/− testes (III; Figure 4D). Besides, a significantly decreased expression of pluripotency factors, such as *Oct4*, *Lin28*, and *Gfra1*, for the stem cell niche function was observed in the SC-*Rb*−/−*E2f3*+/+ testes and finally restored in the SC-*Rb*−/−*E2f3*−/− testes (III; Figure 4E).

Follistatin (*Fst*) is an E2F target gene that is highly expressed in immature testes, whose expression decreases as the animal reaches adulthood [79]. In our model, the

mRNA expression of *Fst* was found to vary depending on the E2F3 status. Namely, it is highly induced in *SC-Rb−/−E2f3+/+* mice and decreased in the *SC-Rb−/−E2f3−/−* mice, suggesting that RB-E2F3 inhibits the expression of *Fst* in WT testes. Interestingly, overexpression of *Fst* in the testis results in alterations in the seminiferous tubule architecture similar to those in *SC-Rb−/−E2f3+/+* and *SC-Rb−/−E2f3+/−* mice [230]. In our model, the high expression of *Fst* in the *SC-Rb−/−E2f3+/+* mice could have contributed to the SC dysfunction. However, as FST inhibits activin A and activin B, which promote SC proliferation [231], increased *Fst* expression could have been a consequence to the cell cycle reentry of adult SCs.

5.3.6 Future perspectives (III)

Traditionally, it has been thought that adult SCs are permanently quiescent and terminally differentiated. However, it has been suggested that, instead, they may be arrested proliferating cells. This is because mouse and human adult SCs have been reported to resume proliferation in culture [232] and to show the expression of several DNA repair proteins after irradiation, such as XRCC1 and PARP1, a phenomenon that has not been observed in other quiescent cells [232–235]. RB-E2F3 may participate in arrested proliferation, but still more studies need to be performed. Furthermore, unknown RB-binding partners to control the proliferation or differentiation of SCs may yet be found.

Among RB and E2F family proteins, functional compensation is observed because they share the same consensus DNA-binding sequence [236]. For example, in our *SC-Rb−/−E2f3+/+* mice, ectopic expression of p107 was observed in adult SCs, which makes the study of the functions of a specific RB or E2F protein *in vivo* challenging.

5.4 Endothelial-specific plasmalemma vesicle-associated protein is needed for normal testicular development (IV)

Previous studies have reported the role of PLVAP in microvasculature permeability, leukocyte migration, angiogenesis of blood vessels, and seeding of fetal monocyte-derived macrophages to different tissues in mice [9,195,196,199,237,238]. However, the function of PLVAP in male fertility has not yet been assessed. In this study, using the *Plvap*^{−/−} mouse line, we demonstrated that PLVAP is expressed in the testicular vasculature of WT adult testes and plays a crucial role in normal testicular development and function.

5.4.1 Testicular phenotype of Plvap⁻/⁻ (IV)

Loss of PLVAP produces a significant decrease in body weight, testis size, and relative testis weight (mg/g) of *Plvap*⁻/⁻ mice at five weeks of age in comparison to the control mice (IV; Figures 1A–1C). Histological analysis of the testis revealed an abnormal seminiferous tubule architecture in the *Plvap*⁻/⁻ testis at five weeks of age. Most of the seminiferous tubule cross sections displayed incomplete spermatogenesis with a reduced number of germ cells and absence of ES layer (IV; Figure 2A). Therefore, it was challenging to identify specific seminiferous epithelium stages. To evaluate whether the germ cell loss in the *Plvap*⁻/⁻ testis is due to increased apoptosis, TUNEL staining analysis at five weeks of age was performed. Notably, the *Plvap*⁻/⁻ testis showed a significantly increased rate of germ cell apoptosis that may contribute to the loss of differentiating cells and smaller testis size in comparison to the control testis (IV; Figures 3A–3C). In line with the observations described above, the cauda epididymis histology of the *Plvap*⁻/⁻ testis at five weeks of age only showed immature germ cells (IV; Figure 2C). Consequently, the *Plvap*⁻/⁻ mice were found to be infertile at the age of five weeks. These data indicate that loss of *Plvap* affects testicular development and impairs spermatogenesis.

5.4.2 Abnormal proliferation of somatic cells in adult Plvap⁻/⁻ mouse testes (IV)

To evaluate whether the abnormal proliferation dynamics of testicular somatic cells is the reason for the decreased testis size and arrested spermatogenesis in the adult *Plvap*⁻/⁻ mice, we used immunofluorescence to evaluate the proliferation rate and number of PTMs, SCs, and Leydig cells at different time points.

Immunofluorescence staining of the α-SMA antibody (a PTM marker) together with KI67 (a proliferation cell marker) antibodies showed that the proliferation rate of PTMs in the *Plvap*⁻/⁻ testes does not change at the age of one week in comparison to the control testes. At two weeks of age, the proliferation rate of PTMs in the *Plvap*⁻/⁻ testes was found to be significantly lower than in the control testis. Interestingly, the proliferation rate of PTMs in the *Plvap*⁻/⁻ testes at the age of five weeks was found to be significantly increased in comparison to the control testes (IV; Figures 5A and 5B). Additionally, the proliferation rate and number of SCs were also evaluated at the same time points. The only significant difference observed in the proliferation rate between the *Plvap*⁻/⁻ and control testes was at the age of two weeks (IV; Figures 5C and 5D). Besides, the BTB integrity observed by ESPIN and CLAUDIN 11 immunostaining showed that their protein expression pattern in *Plvap*⁻/⁻ is comparable to that of the control mice (IV; Supplementary Figure 2). Despite the abnormal proliferation of SCs in the *Plvap*⁻/⁻ testes, their maturation was

not affected as the SCs were quiescent and able to form a BTB at the age of five weeks.

To evaluate whether the proliferation rate and number of Leydig cells were altered in the *Plvap*$^{-/-}$ testes, we performed immunostaining of 3β-HSD (a marker for Leydig cells) and KI67 antibody at two and five weeks of age. Quantification of Leydig cells in proliferation (3β-HSD+KI67+ cells) showed that the proliferation rate was affected in the *Plvap*$^{-/-}$ testes at the age of two weeks. However, similar to SCs, the number of Leydig cells per cross-sectional area was comparable to that in the control mice at the age of five weeks (IV; Figure 6A–6C). These results indicate that the proliferation dynamics of somatic cells are altered in *Plvap*$^{-/-}$ testes.

5.4.3 The testicular phenotype of the *Plvap*$^{-/-}$ adult testis is due to insufficient gonadotropin stimulation (IV)

To evaluate whether the pituitary hormone level contributed to the testicular phenotype, the levels of LH and FSH in the serum and pituitary were measured. Notably, *Plvap*$^{-/-}$ mice were found to have significantly decreased LH and FSH serum levels in comparison to the control mice (IV; Figures 8A and 8B). Interestingly, the intrapituitary hormone levels were also found to be significantly lower in the *Plvap*$^{-/-}$ testes at the age of five weeks (IV; Figures 8C and 8D). Collectively, these data indicate that the testis phenotype in *Plvap*$^{-/-}$ mice is likely due to insufficient gonadotropin stimulation.

5.4.4 Hormonal replacement therapy recovered the *Plvap*-/- phenotype partially (IV)

Hormonal replacement therapy was performed at the age of one to five weeks to evaluate the contribution of hormone deficiency to the testicular phenotype of *Plvap*$^{-/-}$ mice. *Plvap*$^{-/-}$ mice and controls were injected with 1 U of hCG three times a week.

According to the histological analysis of the *Plvap*$^{-/-}$ testis at five weeks of age, most of the seminiferous tubule epithelia were found to exhibit incomplete spermatogenesis, lacking the ES layer. Thus, to evaluate whether hormonal therapy induces the completion of spermatogenesis in the *Plvap*$^{-/-}$ testis, we performed immunofluorescence staining with rhodamine-labeled peanut agglutinin, which stains the acrosome in RSs and ESs. Immunofluorescence staining showed that the phenotype of the hCG-treated *Plvap*$^{-/-}$ testis was partially recovered. Moreover, peanut agglutinin staining showed an increased number of RSs and ESs in the seminiferous epithelium of hCG-treated *Plvap*$^{-/-}$ mice in comparison to untreated *Plvap*$^{-/-}$ mice (IV; Figure 10A). Quantification of the seminiferous tubules

exhibiting complete spermatogenesis or lacking one more layer of RSs or ESs was also was performed. The results show that hCG-treated $Plvap^{-/-}$ mice displayed a significantly increased number of tubules exhibiting complete spermatogenesis and a significantly decreased number of tubules lacking an ES layer in comparison to untreated $Plvap^{-/-}$ mice (IV; Figure 10B). In line with the observations described above, hematoxylin and eosin staining of the cauda epididymis of treated-$Plvap^{-/-}$ mice showed mature spermatozoa (IV; Figure 10C). Collectively, our data show that the testicular phenotype of $Plvap^{-/-}$ mice is mainly due to the abnormal hormone secretion as hormonal therapy was able to partially recover the testicular phenotype of $Plvap^{-/-}$ mice.

The failure of spermatogenesis due to low gonadotrophin levels observed in the $Plvap^{-/-}$ mice has also been reported in other gonadotrophin-related mouse models, in which the significantly low androgen levels affect spermatogenesis. For example, in LH-receptor-deficient mice (LuRKO mice), the ITT levels were found to be significantly lower and the FSH levels were found to be two times higher than in the control mice. Notably, the testes of young adult LuRKO mice have the same size and weight and exhibit narrow seminiferous tubules and spermatogenic arrest as those of $Plvap^{-/-}$ mice [135]. However, the low but detectable ITT levels in LuRKO mice do not completely halt spermatogenesis but rather delay the spermatogenic cycle. Despite the very low ITT levels in the testes of LuRKO mice, the testes of 12-month-old mutant mice display complete spermatogenesis [249]. Therefore, it is important to assess the ITT levels in $Plvap^{-/-}$ testes and whether those levels can maintain spermatogenesis in $Plvap^{-/-}$ testes at an older age, similar to LuRKO mice. In FSHR- [239] or FSHβ-deficient (FSHβR) [240] mice, spermatogenesis is normal and the mice are fertile. However, the testis size and the diameter of the seminiferous tubules are significantly reduced as a result of abnormal SC proliferation during the pubertal age. On the basis of these phenotypes, the abnormal proliferation dynamics of SCs in $Plvap^{-/-}$ testes may be explained by the significantly reduced levels of FSH in serum, which lowers the proliferation of SCs at the pubertal age and, consequently, results in a small testis size at the age of five weeks.

It has been shown that PLVAP controls the seeding of fetal liver-derived macrophages and that $Plvap^{-/-}$ mice have a diminished population of these macrophages in the spleen, peritoneal cavity, mammary glands, and lungs [10,250]. Besides, it has previously been reported that testicular macrophages regulate the development and function of Leydig cells [241,242]. In our study, we did not examine the testicular macrophage composition in $Plvap^{-/-}$. Hence, it is important to verify whether $Plvap^{-/-}$ testes lack this specific macrophage population. If this is the case, then the $Plvap^{-/-}$ mouse line would be a unique model to study the role of this specific macrophage population in the testicular function.

5.4.5   Future perspectives (IV)

To our knowledge, this is the first study describing the role of PLVAP in the endocrine regulation of the testis. Since the hCG treatment was able to partially recover the phenotype of the *Plvap*$^{-/-}$ testis, we concluded that the gonadotropin insufficiency is the main cause of the spermatogenesis failure. However, since a global *Plvap* knockout model was used, indirect factors such as leakage of plasma proteins into the testis, may also contribute to the *Plvap*$^{-/-}$ testis dysfunction.

Interestingly, as the pituitary of *Plvap*$^{-/-}$ mice also displays low levels of LH and FSH, the *Plvap* deficiency has evident impact on the gonadotropin production. Further studies are needed to determine the impact of the *Plvap* deficiency on the pituitary development and function.

It has been proposed that PLVAP is a potential therapeutic target for some forms of cancer treatment as it decreases tumor growth and has minor systemic toxicity [200]. However, in this study, we have shown that the loss of PLVAP also has adverse effects on the endocrine regulation of the testis. Thus, further studies on characterizing the effect of the partial loss of *Plvap* need to be performed.

6 Conclusions

Collectively, the results of this thesis study addressed the role of selected proteins in controlling specific events during testicular development and spermatogenesis. We also developed a flow-cytometry-based method for the study of testis composition. This study contributes with key information for a better understanding of the molecular processes that affect male fertility and reproduction.

The main findings of the studies performed herein are as follows:

I.   The flow cytometry protocol established in this study is a great tool for studying rodent testicular cell composition. Moreover, this protocol is very advantageous because multiple intracellular markers can be used and samples can be stored and delivered to other laboratories.

II. USF1 is a transcription factor involved in maintaining the balance between spermatogonial cell renewal and differentiation in the mouse testis.

III. Both RB and the transcription factor E2F3 are implicated in the maintenance of adult SCs in a quiescent state.

IV. PLVAP contributes indirectly to normal testicular development and function by influencing the endocrine regulation of the testis.

Acknowledgements

to Finland and gave me the greatest and unforgettable opportunity in my career and personal development. Also, I would like to thank the University of Turku Graduate School UTUGS, Turku Doctoral Programme of Molecular Medicine (TuDMM), Jalmari ja Rauha Ahokas Foundation, and Lounais-Suomen Syöpäyhdistys for the financial contribution to support my work during these years.

My work was performed in a functional working environment with professors, senior researchers, postdocs, Ph.D. students, master students, summer students, administrative staff, and technicians. This proper environment is successfully managed by Dr. Tuula Hämäläinen, Ph.D. Thank you! For creating a nice environment to do science, and reminding us every Monday meeting to keep the lab tidy. I want to thank Assistant Professor Noora Kotaja, Ph.D., Professor Matti Poutanen, Ph.D., Docent Helena Virtanen, M.D., Ph.D. Docent Leena Strauss, Ph.D., Docent Jukka Kero, M.D., Adjunct Professor Petra Sipilä, Ph.D., and Adjunct Professor Nafis Rahman M.D., Ph.D., for your constructive critical feedback during the Wednesday seminars.

During my years at the IPP department, I had the pleasure to meet a lot of talented and passionate people who became very close to me and without their help, my Ph.D. path would have been much more challenging and probably impossible.

Firstly, I wish to thank Dr. Juho Antti-Mäkelä, Ph.D. You patiently supervised my first steps in growing into a scientist when I first came to the IPP in 2013 for a short internship. When I think back, I have to mention that it is impressive how you were really brave to deal with my Spanglish skills. During my last years of PhD, your ideas and insights made it much easier to proceed in the right direction and complete this PhD project successfully.

I would like to specially thank Associate Professor Adolfo Rivero-Müller, Ph.D. I was relieved to know that a Spanish speaking researcher was working in the IPP department when I first came. Without your expertise and help, I would have struggled a lot.

The best officemates I could think Dr. Gabriela Martinez Chacón, Ph.D., and Wiwat Rodpraset, M.D. Thank you for the great company, gym, movie nights, karaoke, trips together, encouraging talks, and also probably tough times because none PhD roads are easy. While we might no longer be colleagues at work, you will never stop being my friends.

I wish to express my special gratitude to Tiina Lehtiniemi, M.Sc., and Michael Gabriel, M.D. for the scientific and non-scientific experiences we have spent together in the lab and outdoors. For all those dancing nights at Forte, movie recording, and editing in the B602 office, and especially for being such supportive friends during all my troublesome days.

I wish to thank all past and present colleagues in the department: Opeyemi Olotu, Jaakko Koskeniemi, Hanna Heikelä, Mari Lehti, Riikka Huhtaniemi, Valeriy

Gutierrez Quequezana, Anita Santana Sánchez, Victor Solis Mezarino, and Joel More for many memorable Peruvian celebrations!

In Peru, I wish to thank my aunt Eli, uncle Grover, and Miguel, for always being very emotionally supportive of me and for taking good care of my loved ones when I am not there. Thank you "*sangrecita*" for always making me laugh. Finally, I owe my deepest gratitude and love to my family, my parents Marino Cisneros Vásquez, Graciela Montalvo Quiñones, and my brother Jean Pierre Cisneros Montalvo. A part of my heart has been there with you all this time, and your unconditional love, support, and trust give me strength and resilience every day to follow my dreams. You are my best example of commitment and that hard work pays off. Los amo.

Turku, November 2020

Sheyla Cisneros Montalvo

References

1. Fainberg J, Kashanian JA. Recent advances in understanding and managing male infertility [version 1; peer review: 3 approved]. *F1000Research*. 2019;8(670).
2. Boivin J, Bunting L, Collins JA, Nygren KG. International estimates of infertility prevalence and treatment-seeking: Potential need and demand for infertility medical care. *Hum Reprod*. 2007;22(6):1506-1512.
3. Cavallini G. Male idiopathic oligoasthenoteratozoospermia. *Asian J Androl*. 2006;8(2):143-157.
4. Guo J, Fang W, Chen X, et al. Upstream stimulating factor 1 suppresses autophagy and hepatic lipid droplet catabolism by activating mTOR. *FEBS Lett*. 2018;592(16):2725-2738.
5. Pajukanta P, Lilja HE, Sinsheimer JS, et al. Familial combined hyperlipidemia is associated with upstream transcription factor 1 (USF1). *Nat Genet*. 2004;36(4):371-376.
6. Laurila PP, Soronen J, Kooijman S, et al. USF1 deficiency activates brown adipose tissue and improves cardiometabolic health. *Sci Transl Med*. 2016;8(323):323ra13.
7. Engel BE, Cress WD, Santiago-Cardona PG. The retinoblastoma protein: A master tumor suppressor acts as a link between cell cycle and cell adhesion. *Cell Health Cytoskelet*. 2015;7:1-10.
8. Rotgers E, Rivero-Muller A, Nurmio M, et al. Retinoblastoma protein (RB) interacts with E2F3 to control terminal differentiation of sertoli cells. *Cell Death Dis*. 2014;5:e1274.
9. Stan RV, Tse D, Deharvengt SJ, et al. The diaphragms of fenestrated endothelia: Gatekeepers of vascular permeability and blood composition. *Dev Cell*. 2012;23(6):1203-1218.
10. Rantakari P, Jäppinen N, Lokka E, et al. Fetal liver endothelium regulates the seeding of tissue-resident macrophages. *Nature*. 2016;538(7625):392-396.
11. Karl J, Capel B. Sertoli cells of the mouse testis originate from the coelomic epithelium. *Developmental Biology*. 1998;203(2):323-333. doi: https://doi.org/10.1006/dbio.1998.9068.
12. Schmahl J, Eicher EM, Washburn LL, Capel B. Sry induces cell proliferation in the mouse gonad. *Development*. 2000;127(1):65-73.
13. Barton LJ, LeBlanc MG, Lehmann R. Finding their way: Themes in germ cell migration. *Curr Opin Cell Biol*. 2016;42:128-137.
14. Hanley NA, Hagan DM, Clement-Jones M, et al. SRY, SOX9, and DAX1 expression patterns during human sex determination and gonadal development. *Mech Dev*. 2000;91(1-2):403-407.
15. Koopman P, Munsterberg A, Capel B, Vivian N, Lovell-Badge R. Expression of a candidate sex-determining gene during mouse testis differentiation. *Nature*. 1990;348(6300):450-452.
16. Hacker A, Capel B, Goodfellow P, Lovell-Badge R. Expression of sry, the mouse sex determining gene. *Development*. 1995;121(6):1603-1614.
17. Sekido R, Bar I, Narvaez V, Penny G, Lovell-Badge R. SOX9 is up-regulated by the transient expression of SRY specifically in sertoli cell precursors. *Dev Biol*. 2004;274(2):271-279.
18. Nel-Themaat L, Vadakkan TJ, Wang Y, Dickinson ME, Akiyama H, Behringer RR. Morphometric analysis of testis cord formation in Sox9-EGFP mice. *Dev Dyn*. 2009;238(5):1100-1110.
19. Munsterberg A, Lovell-Badge R. Expression of the mouse anti-mullerian hormone gene suggests a role in both male and female sexual differentiation. *Development*. 1991;113(2):613-624.

20. Griswold SL, Behringer RR. Fetal leydig cell origin and development. *Sex Dev*. 2009;3(1):1-15.

21. Hilscher B, Hilscher W, Bulthoff-Ohnolz B, et al. Kinetics of gametogenesis. I. comparative histological and autoradiographic studies of oocytes and transitional prospermatogonia during oogenesis and prespermatogenesis. *Cell Tissue Res*. 1974;154(4):443-470.

22. Vergouwen RP, Jacobs SG, Huiskamp R, Davids JA, de Rooij DG. Proliferative activity of gonocytes, sertoli cells and interstitial cells during testicular development in mice. *J Reprod Fertil*. 1991;93(1):233-243.

23. Koubova J, Menke DB, Zhou Q, Capel B, Griswold MD, Page DC. Retinoic acid regulates sex-specific timing of meiotic initiation in mice. *Proc Natl Acad Sci U S A*. 2006;103(8):2474-2479.

24. Bowles J, Feng CW, Spiller C, Davidson TL, Jackson A, Koopman P. FGF9 suppresses meiosis and promotes male germ cell fate in mice. *Dev Cell*. 2010;19(3):440-449.

25. Nurmio M, Toppari J, Zaman F, et al. Inhibition of tyrosine kinases PDGFR and C-kit by imatinib mesylate interferes with postnatal testicular development in the rat. *Int J Androl*. 2007;30(4):366-76; discussion 376.

26. Orth JM, Qiu J, Jester WF,Jr, Pilder S. Expression of the c-kit gene is critical for migration of neonatal rat gonocytes in vitro. *Biol Reprod*. 1997;57(3):676-683.

27. Basciani S, De Luca G, Dolci S, et al. Platelet-derived growth factor receptor beta-subtype regulates proliferation and migration of gonocytes. *Endocrinology*. 2008;149(12):6226-6235.

28. Manku G, Culty M. Mammalian gonocyte and spermatogonia differentiation: Recent advances and remaining challenges. *Reproduction*. 2015;149(3):R139-57.

29. Bellvé A,R., Cavicchia JC, Milletfe CF, Brien DAO, Bhatnagar YM, Dym M. Spermatogenic cells of the prepuberal mouse: Isolation and morphological characterization. *J Cell Biol*. 1977;74:68-85.

30. Griswold MD. Interactions between germ cells and sertoli cells in the testis. *Biol Reprod*. 1995;52(2):211-216.

31. Meng X, Lindahl M, Hyvonen ME, et al. Regulation of cell fate decision of undifferentiated spermatogonia by GDNF. *Science*. 2000;287(5457):1489-1493.

32. Sharma M, Braun RE. Cyclical expression of GDNF is required for spermatogonial stem cell homeostasis. *Development*. 2018;145(5):10.1242/dev.151555.

33. Chen LY, Willis WD, Eddy EM. Targeting the gdnf gene in peritubular myoid cells disrupts undifferentiated spermatogonial cell development. *Proc Natl Acad Sci U S A*. 2016;113(7):1829-1834.

34. Bhang DH, Kim B, Kim BG, et al. Testicular endothelial cells are a critical population in the germline stem cell niche. *Nature Communications*. 2018;9(1):4379.

35. Buaas FW, Kirsh AL, Sharma M, et al. Plzf is required in adult male germ cells for stem cell self-renewal. *Nat Genet*. 2004;36(6):647-652.

36. Costoya JA, Hobbs RM, Barna M, et al. Essential role of plzf in maintenance of spermatogonial stem cells. *Nat Genet*. 2004;36(6):653-659.

37. Falender AE, Freiman RN, Geles KG, et al. Maintenance of spermatogenesis requires TAF4b, a gonad-specific subunit of TFIID. *Genes Dev*. 2005;19(7):794-803.

38. Hobbs RM, Fagoonee S, Papa A, et al. Functional antagonism between Sall4 and plzf defines germline progenitors. *Cell Stem Cell*. 2012;10(3):284-298.

39. Chan AL, La HM, Legrand JMD, et al. Germline stem cell activity is sustained by SALL4-dependent silencing of distinct tumor suppressor genes. *Stem Cell Reports*. 2017;9(3):956-971.

40. Goertz MJ, Wu Z, Gallardo TD, Hamra FK, Castrillon DH. Foxo1 is required in mouse spermatogonial stem cells for their maintenance and the initiation of spermatogenesis. *J Clin Invest*. 2011;121(9):3456-3466.

41. Huckins C. The spermatogonial stem cell population in adult rats. I. their morphology, proliferation and maturation. *Anat Rec*. 1971;169(3):533-557.

42. de Rooij DG. The nature and dynamics of spermatogonial stem cells. *Development*. 2017;144(17):3022-3030.

43. Lord T, Oatley JM. A revised asingle model to explain stem cell dynamics in the mouse male germline. *Reproduction*. 2017;154(2):R55-R64.

44. Mäkelä J, Toppari J. Spermatogenic cell syncytium. . 2018:124-133. doi: https://doi.org/10.1016/B978-0-12-801238-3.64569-5.

45. de Rooij DG. The nature and dynamics of spermatogonial stem cells. *Development*. 2017;144(17):3022-3030.

46. Busada JT, Geyer CB. The role of retinoic acid (RA) in spermatogonial differentiation. *Biol Reprod*. 2016;94(1):10.

47. Sugimoto R, Nabeshima Y, Yoshida S. Retinoic acid metabolism links the periodical differentiation of germ cells with the cycle of sertoli cells in mouse seminiferous epithelium. *Mech Dev*. 2012;128(11-12):610-624.

48. de Rooij DG, Russell LD. All you wanted to know about spermatogonia but were afraid to ask. *J Androl*. 2000;21(6):776-798.

49. Russell LD, Clermont Y. Degeneration of germ cells in normal, hypophysectomized and hormone treated hypophysectomized rats. *Anat Rec*. 1977;187(3):347-366.

50. Baudat F, Manova K, Yuen JP, Jasin M, Keeney S. Chromosome synapsis defects and sexually dimorphic meiotic progression in mice lacking Spo11. *Mol Cell*. 2000;6(5):989-998.

51. Yoshida K, Kondoh G, Matsuda Y, Habu T, Nishimune Y, Morita T. The mouse RecA-like gene Dmc1 is required for homologous chromosome synapsis during meiosis. *Mol Cell*. 1998;1(5):707-718.

52. Watanabe Y, Nurse P. Cohesin Rec8 is required for reductional chromosome segregation at meiosis. *Nature*. 1999;400(6743):461-464.

53. Yuan L, Liu JG, Zhao J, Brundell E, Daneholt B, Hoog C. The murine SCP3 gene is required for synaptonemal complex assembly, chromosome synapsis, and male fertility. *Mol Cell*. 2000;5(1):73-83.

54. Revenkova E, Eijpe M, Heyting C, et al. Cohesin SMC1 beta is required for meiotic chromosome dynamics, sister chromatid cohesion and DNA recombination. *Nat Cell Biol*. 2004;6(6):555-562.

55. Anderson EL, Baltus AE, Roepers-Gajadien HL, et al. Stra8 and its inducer, retinoic acid, regulate meiotic initiation in both spermatogenesis and oogenesis in mice. *Proc Natl Acad Sci U S A*. 2008;105(39):14976-14980.

56. Zhou Q, Li Y, Nie R, et al. Expression of stimulated by retinoic acid gene 8 (Stra8) and maturation of murine gonocytes and spermatogonia induced by retinoic acid in vitro. *Biol Reprod*. 2008;78(3):537-545.

57. Oulad-Abdelghani M, Bouillet P, Decimo D, et al. Characterization of a premeiotic germ cell-specific cytoplasmic protein encoded by Stra8, a novel retinoic acid-responsive gene. *J Cell Biol*. 1996;135(2):469-477.

58. Brunn v. Beiträge zur entwicklungsgeschichte der samenkörper. *Arch Mikrosk Anat*. 1976;12:528-536.

59. Meikar O, Vagin VV, Chalmel F, et al. An atlas of chromatoid body components. *RNA*. 2014;20(4):483-495.

60. Guyonnet B, Dacheux F, Dacheux JL, Gatti JL. The epididymal transcriptome and proteome provide some insights into new epididymal regulations. *J Androl*. 2011;32(6):651-664.

61. Gervasi MG, Visconti PE. Molecular changes and signaling events occurring in spermatozoa during epididymal maturation. *Andrology*. 2017;5(2):204-218.

62. Oakberg EF. Duration of spermatogenesis in the mouse and timing of stages of the cycle of the seminiferous epithelium. *Am J Anat*. 1956;99(3):507-516.

63. Leblond CP, Clermont Y. Definition of the stages of the cycle of the seminiferous epithelium in the rat. *Ann N Y Acad Sci*. 1952;55(4):548-573.

64. Toppari J, Parvinen M. In vitro differentiation of rat seminiferous tubular segments from defined stages of the epithelial cycle morphologic and immunolocalization analysis. *J Androl*. 1985;6(6):334-343.

65. Clermont Y. The cycle of the seminiferous epithelium in man. *Am J Anat*. 1963;112:35-51.

66. Heller CH, Clermont Y. Kinetics of the germinal epithelium in man. *Recent Prog Horm Res*. 1964;20:545-575.

67. Muciaccia B, Boitani C, Berloco BP, et al. Novel stage classification of human spermatogenesis based on acrosome development. *Biol Reprod*. 2013;89(3):60.

68. Kotaja N, Kimmins S, Brancorsini S, et al. Preparation, isolation and characterization of stage-specific spermatogenic cells for cellular and molecular analysis. *Nat Methods*. 2004;1(3):249-254.

69. Toppari J. *Rat spermatogenesis in vitro :: Studies on differentiation of seminiferous tubule segments at defined stages of the epithelial cycle.* Turku : J. Toppari,; 1986:72, [56].

70. Clermont Y, Trott M. Duration of the cycle of the seminiferous epithelium in the mouse and hamster determined by means of 3H-thymidine and radioautography. *Fertil Steril*. 1969;20(5):805-817.

71. Orth JM. Proliferation of sertoli cells in fetal and postnatal rats: A quantitative autoradiographic study. *Anat Rec*. 1982;203(4):485-492.

72. O'Shaughnessy PJ, Monteiro A, Abel M. Testicular development in mice lacking receptors for follicle stimulating hormone and androgen. *PLoS One*. 2012;7(4):e35136.

73. Orth JM. The role of follicle-stimulating hormone in controlling sertoli cell proliferation in testes of fetal rats. *Endocrinology*. 1984;115(4):1248-1255.

74. Singh J, Handelsman DJ. Neonatal administration of FSH increases sertoli cell numbers and spermatogenesis in gonadotropin-deficient (hpg) mice. *J Endocrinol*. 1996;151(1):37-48.

75. Grinspon RP, Bedecarras P, Ballerini MG, et al. Early onset of primary hypogonadism revealed by serum anti-mullerian hormone determination during infancy and childhood in trisomy 21. *Int J Androl*. 2011;34(5 Pt 2):e487-98.

76. Rey R, Lukas-Croisier C, Lasala C, Bedecarrás P. AMH/MIS: What we know already about the gene, the protein and its regulation. *Mol Cell Endocrinol*. 2003;211(1–2):21-31.

77. Anderson RA, Cambray N, Hartley PS, McNeilly AS. Expression and localization of inhibin alpha, inhibin/activin betaA and betaB and the activin type II and inhibin beta-glycan receptors in the developing human testis. *Reproduction*. 2002;123(6):779-788.

78. Archambeault DR, Yao HH. Activin A, a product of fetal leydig cells, is a unique paracrine regulator of sertoli cell proliferation and fetal testis cord expansion. *Proc Natl Acad Sci U S A*. 2010;107(23):10526-10531.

79. Barakat B, O'Connor AE, Gold E, de Kretser DM, Loveland KL. Inhibin, activin, follistatin and FSH serum levels and testicular production are highly modulated during the first spermatogenic wave in mice. *Reproduction*. 2008;136(3):345-359.

80. Mendis SH, Meachem SJ, Sarraj MA, Loveland KL. Activin A balances sertoli and germ cell proliferation in the fetal mouse testis. *Biol Reprod*. 2011;84(2):379-391.

81. Cudicini C, Lejeune H, Gomez E, et al. Human leydig cells and sertoli cells are producers of interleukins-1 and -6. *J Clin Endocrinol Metab*. 1997;82(5):1426-1433.

82. Hayrabedyan S, Todorova K, Jabeen A, et al. Sertoli cells have a functional NALP3 inflammasome that can modulate autophagy and cytokine production. *Sci Rep*. 2016;6:18896.

83. Hayes R, Chalmers SA, Nikolic-Paterson DJ, Atkins RC, Hedger MP. Secretion of bioactive interleukin 1 by rat testicular macrophages in vitro. *J Androl*. 1996;17(1):41-49.

84. Lin T, Wang D, Nagpal ML. Human chorionic gonadotropin induces interleukin-1 gene expression in rat leydig cells in vivo. *Mol Cell Endocrinol*. 1993;95(1-2):139-145.

85. Wang DL, Nagpal ML, Calkins JH, Chang WW, Sigel MM, Lin T. Interleukin-1 beta induces interleukin-1 alpha messenger ribonucleic acid expression in primary cultures of leydig cells. *Endocrinology*. 1991;129(6):2862-2866.

86. Gerard N, Syed V, Bardin W, Genetet N, Jegou B. Sertoli cells are the site of interleukin-1 alpha synthesis in rat testis. *Mol Cell Endocrinol*. 1991;82(1):R13-6.

87. Petersen C, Svechnikov K, Froysa B, Soder O. The p38 MAPK pathway mediates interleukin-1-induced sertoli cell proliferation. *Cytokine*. 2005;32(1):51-59.

88. Smith LB, Walker WH. The regulation of spermatogenesis by androgens. *Semin Cell Dev Biol*. 2014;30:2-13.

89. Bremner WJ, Millar MR, Sharpe RM, Saunders PT. Immunohistochemical localization of androgen receptors in the rat testis: Evidence for stage-dependent expression and regulation by androgens. *Endocrinology*. 1994;135(3):1227-1234.

90. You L, Sar M. Androgen receptor expression in the testes and epididymides of prenatal and postnatal sprague-dawley rats. *Endocrine*. 1998;9(3):253-261.

91. Hazra R, Corcoran L, Robson M, et al. Temporal role of sertoli cell androgen receptor expression in spermatogenic development. *Mol Endocrinol*. 2013;27(1):12-24.

92. Beumer TL, Kiyokawa H, Roepers-Gajadien HL, et al. Regulatory role of p27kip1 in the mouse and human testis. *Endocrinology*. 1999;140(4):1834-1840.

93. Polyak K, Lee MH, Erdjument-Bromage H, et al. Cloning of p27Kip1, a cyclin-dependent kinase inhibitor and a potential mediator of extracellular antimitogenic signals. *Cell*. 1994;78(1):59-66.

94. Holsberger DR, Cooke PS. Understanding the role of thyroid hormone in sertoli cell development: A mechanistic hypothesis. *Cell Tissue Res*. 2005;322(1):133-40.

95. Gilleron J, Nebout M, Scarabelli L, et al. A potential novel mechanism involving connexin 43 gap junction for control of sertoli cell proliferation by thyroid hormones. *J Cell Physiol*. 2006;209(1):153-161.

96. Fumel B, Guerquin MJ, Livera G, et al. Thyroid hormone limits postnatal sertoli cell proliferation in vivo by activation of its alpha1 isoform receptor (TRalpha1) present in these cells and by regulation of Cdk4/JunD/c-myc mRNA levels in mice. *Biol Reprod*. 2012;87(1):16, 1-9.

97. Mruk DD, Cheng CY. Sertoli-sertoli and sertoli-germ cell interactions and their significance in germ cell movement in the seminiferous epithelium during spermatogenesis. *Endocr Rev*. 2004;25(5):747-806.

98. Nakanishi Y, Shiratsuchi A. Phagocytic removal of apoptotic spermatogenic cells by sertoli cells: Mechanisms and consequences. *Biol Pharm Bull*. 2004;27(1):13-16.

99. Berruti G, Paiardi C. The dynamic of the apical ectoplasmic specialization between spermatids and sertoli cells: The case of the small GTPase Rap1. *Biomed Res Int*. 2014;2014:635979.

100. Brennan J, Karl J, Capel B. Divergent vascular mechanisms downstream of sry establish the arterial system in the XY gonad. *Dev Biol*. 2002;244(2):418-428.

101. Coveney D, Cool J, Oliver T, Capel B. Four-dimensional analysis of vascularization during primary development of an organ, the gonad. *Proc Natl Acad Sci USA*. 2008;105(20):7212-7217.

102. Gat Y, Gornish M, Perlow A, et al. Azoospermia and sertoli-cell-only syndrome: Hypoxia in the sperm production site due to impairment in venous drainage of male reproductive system. *Andrologia*. 2010;42(5):314-321.

103. Silber S. Blood supply to the testis. In: Silber S, ed. *Fundamentals of male infertility*. Cham: Springer International Publishing; 2018:25-27. https://doi.org/10.1007/978-3-319-76523-5_5. 10.1007/978-3-319-76523-5_5.

104. Damber JE, Janson PO. Testicular blood flow and testosterone concentration in spermatic venous blood of anaesthetized rats. *J Reprod Fertil*. 1978;52(2):265-269.

105. Damber JE, Maddocks S, Widmark A, Bergh A. Testicular blood flow and vasomotion can be maintained by testosterone in leydig cell-depleted rats. *Int J Androl*. 1992;15(5):385-393.

106. Welsh M, Sharpe RM, Moffat L, et al. Androgen action via testicular arteriole smooth muscle cells is important for leydig cell function, vasomotion and testicular fluid dynamics. *PLoS One*. 2010;5(10):e13632.

107. Aird WC. Endothelial cell heterogeneity. *Cold Spring Harb Perspect Med*. 2012;2(1):a006429.

108. Kim YH, Oh MG, Bhang DH, et al. Testicular endothelial cells promote self-renewal of spermatogonial stem cells in ratsdagger. *Biol Reprod*. 2019;101(2):360-367.

109. Haider SG. Cell biology of leydig cells in the testis. *Int Rev Cytol*. 2004;233:181-241.

110. Yao HH, Whoriskey W, Capel B. Desert hedgehog/patched 1 signaling specifies fetal leydig cell fate in testis organogenesis. *Genes Dev*. 2002;16(11):1433-1440.

111. Huhtaniemi I, Pelliniemi LJ. Fetal leydig cells: Cellular origin, morphology, life span, and special functional features. *Proc Soc Exp Biol Med*. 1992;201(2):125-140.

112. Ye L, Li X, Li L, Chen H, Ge RS. Insights into the development of the adult leydig cell lineage from stem leydig cells. *Front Physiol*. 2017;8:430.

113. Shima Y, Matsuzaki S, Miyabayashi K, et al. Fetal leydig cells persist as an androgen-independent subpopulation in the postnatal testis. *Mol Endocrinol*. 2015;29(11):1581-1593.

114. O'Shaughnessy PJ, Baker PJ, Heikkila M, Vainio S, McMahon AP. Localization of 17beta-hydroxysteroid dehydrogenase/17-ketosteroid reductase isoform expression in the developing mouse testis--androstenedione is the major androgen secreted by fetal/neonatal leydig cells. *Endocrinology*. 2000;141(7):2631-2637.

115. Winnall WR, Hedger MP. Phenotypic and functional heterogeneity of the testicular macrophage population: A new regulatory model. *J Reprod Immunol*. 2013;97(2):147-158.

116. Niemi M, Sharpe RM, Brown WRA. Macrophages in the interstitial tissue of the rat testis. *Cell Tissue Res*. 1986;243(2):337-344.

117. Itoh M, De Rooij DG, Jansen A, Drexhage HA. Phenotypical heterogeneity of testicular macrophages/dendritic cells in normal adult mice: An immunohistochemical study. *J Reprod Immunol*. 1995;28(3):217-232.

118. Fijak M, Meinhardt A. The testis in immune privilege. *Immunol Rev*. 2006;213:66-81.

119. Wynn TA, Chawla A, Pollard JW. Macrophage biology in development, homeostasis and disease. *Nature*. 2013;496(7446):445-455.

120. Smith LB, O'Shaughnessy PJ, Rebourcet D. Cell-specific ablation in the testis: What have we learned? *Andrology*. 2015;3(6):1035-1049.

121. Hutson JC. Interactions between testicular macrophages and leydig cells. *J Androl*. 1998;19(4):394-398.

122. DeFalco T, Potter SJ, Williams AV, Waller B, Kan MJ, Capel B. Macrophages contribute to the spermatogonial niche in the adult testis. *Cell Rep*. 2015;12(7):1107-1119.

123. DeFalco T, Bhattacharya I, Williams AV, Sams DM, Capel B. Yolk-sac-derived macrophages regulate fetal testis vascularization and morphogenesis. *Proc Natl Acad Sci U S A*. 2014;111(23):E2384-93.

124. Mossadegh-Keller N, Gentek R, Gimenez G, Bigot S, Mailfert S, Sieweke MH. Developmental origin and maintenance of distinct testicular macrophage populations. *J Exp Med*. 2017;214(10):2829-2841.

125. Jeanes A, Wilhelm D, Wilson MJ, et al. Evaluation of candidate markers for the peritubular myoid cell lineage in the developing mouse testis. *Reproduction*. 2005;130(4):509-516.

126. Nurmio M, Kallio J, Adam M, Mayerhofer A, Toppari J, Jahnukainen K. Peritubular myoid cells have a role in postnatal testicular growth. *Spermatogenesis*. 2012;2(2):79-87.

127. Albrecht M. Insights into the nature of human testicular peritubular cells. *Ann Anat*. 2009;191(6):532-540.

128. Skinner MK, Tung PS, Fritz IB. Cooperativity between sertoli cells and testicular peritubular cells in the production and deposition of extracellular matrix components. *J Cell Biol*. 1985;100(6):1941-1947.

129. Chen LY, Brown PR, Willis WB, Eddy EM. Peritubular myoid cells participate in male mouse spermatogonial stem cell maintenance. *Endocrinology*. 2014;155(12):4964-4974.

130. Allan CM, Garcia A, Spaliviero J, et al. Complete sertoli cell proliferation induced by follicle-stimulating hormone (FSH) independently of luteinizing hormone activity: Evidence from genetic models of isolated FSH action. *Endocrinology*. 2004;145(4):1587-1593.

131. Meachem SJ, Nieschlag E, Simoni M. Inhibin B in male reproduction: Pathophysiology and clinical relevance. *Eur J Endocrinol*. 2001;145(5):561-571.

132. Li Y, Schang G, Wang Y, et al. Conditional deletion of FOXL2 and SMAD4 in gonadotropes of adult mice causes isolated FSH deficiency. . 2018;159:2641.

133. Dierich A, Sairam MR, Monaco L, et al. Impairing follicle-stimulating hormone (FSH) signaling in vivo: Targeted disruption of the FSH receptor leads to aberrant gametogenesis and hormonal imbalance. *Proc Natl Acad Sci U S A*. 1998;95(23):13612-13617.

134. Oduwole OO, Peltoketo H, Huhtaniemi IT. Role of follicle-stimulating hormone in spermatogenesis. *Frontiers in Endocrinology*. 2018;9:763.

135. Zhang FP, Poutanen M, Wilbertz J, Huhtaniemi I. Normal prenatal but arrested postnatal sexual development of luteinizing hormone receptor knockout (LuRKO) mice. *Mol Endocrinol*. 2001;15(1):172-183.

136. Lei ZM, Mishra S, Zou W, et al. Targeted disruption of luteinizing hormone/human chorionic gonadotropin receptor gene. *Mol Endocrinol*. 2001;15(1):184-200.

137. Aravindan GR, Ravindranath N, Gopalakrishnan K, Moudgal NR. DNA flow-cytometric analysis of testicular germ cell populations of the bonnet monkey (*macaca radiata*) as a function of sexual maturity. *J Reprod Fertil*. 1990;89(2):397-406.

138. Toppari J, Bishop PC, Parker JW, diZerega GS. DNA flow cytometric analysis of mouse seminiferous epithelium. *Cytometry*. 1988;9(5):456-462.

139. Toppari J, Eerola E, Parvinen M. Flow cytometric DNA analysis of defined stages of rat seminiferous epithelial cycle during in vitro differentiation. *J Androl*. 1985;6(6):325-333.

140. Suresh R, Aravindan GR, Moudgal NR. Quantitation of spermatogenesis by DNA flow cytometry: Comparative study among six species of mammals. *J Biosci*. 1992;17(4):413-419.

141. Baksi A, Vasan SS, Dighe RR. DNA flow cytometric analysis of the human testicular tissues to investigate the status of spermatogenesis in azoospermic patients. *Scientific Reports*. 2018;8(1):11117.

142. La HM, Chan AL, Legrand JMD, et al. GILZ-dependent modulation of mTORC1 regulates spermatogonial maintenance. *Development*. 2018;145(18):10.1242/dev.165324.

143. Finak G, Jiang W, Krouse K, et al. High-throughput flow cytometry data normalization for clinical trials. *Cytometry A*. 2014;85(3):277-286.

144. Hahne F, Khodabakhshi AH, Bashashati A, et al. Per-channel basis normalization methods for flow cytometry data. *Cytometry A*. 2010;77(2):121-131.

145. Zebedee Z, Hara E. Id proteins in cell cycle control and cellular senescence. *Oncogene*. 2001;20(58):8317-8325.

146. Wood MA, Walker WH. USF1/2 transcription factor DNA-binding activity is induced during rat sertoli cell differentiation. *Biol Reprod*. 2009;80(1):24-33.

147. Sawadogo M, Roeder RG. Interaction of a gene-specific transcription factor with the adenovirus major late promoter upstream of the TATA box region. *Cell*. 1985;43(1):165-175.

148. Lefrancois-Martinez AM, Martinez A, Antoine B, Raymondjean M, Kahn A. Upstream stimulatory factor proteins are major components of the glucose response complex of the L-type pyruvate kinase gene promoter. *J Biol Chem*. 1995;270(6):2640-2643.

149. Wang D, Sul HS. Upstream stimulatory factors bind to insulin response sequence of the fatty acid synthase promoter. USF1 is regulated. *J Biol Chem*. 1995;270(48):28716-28722.

150. Huertas-Vazquez A, Aguilar-Salinas C, Lusis AJ, et al. Familial combined hyperlipidemia in mexicans: Association with upstream transcription factor 1 and linkage on chromosome 16q24.1. *Arterioscler Thromb Vasc Biol*. 2005;25(9):1985-1991.

151. Laurila PP, Naukkarinen J, Kristiansson K, et al. Genetic association and interaction analysis of USF1 and APOA5 on lipid levels and atherosclerosis. *Arterioscler Thromb Vasc Biol*. 2010;30(2):346-352.

152. Putt W, Palmen J, Nicaud V, et al. Variation in USF1 shows haplotype effects, gene : Gene and gene : Environment associations with glucose and lipid parameters in the european atherosclerosis research study II. *Hum Mol Genet*. 2004;13(15):1587-1597.

153. Kristiansson K, Ilveskoski E, Lehtimäki T, Peltonen L, Perola M, Karhunen PJ. Association analysis of allelic variants of USF1 in coronary atherosclerosis. *Arterioscler Thromb Vasc Biol*. 2008;28(5):983-989.

154. Komulainen K, Alanne M, Auro K, et al. Risk alleles of USF1 gene predict cardiovascular disease of women in two prospective studies. *PLoS Genet*. 2006;2(5):e69.

155. Auro K, Kristiansson K, Zethelius B, et al. USF1 gene variants contribute to metabolic traits in men in a longitudinal 32-year follow-up study. *Diabetologia*. 2008;51(3):464-472.

156. Choquette AC, Bouchard L, Houde A, Bouchard C, Perusse L, Vohl MC. Associations between USF1 gene variants and cardiovascular risk factors in the quebec family study. *Clin Genet*. 2007;71(3):245-253.

157. Ng MC, Miyake K, So WY, et al. The linkage and association of the gene encoding upstream stimulatory factor 1 with type 2 diabetes and metabolic syndrome in the chinese population. *Diabetologia*. 2005;48(10):2018-2024.

158. Li P, Wang H, Hou M, Li D, Bai H. Upstream stimulating factor1 (USF1) enhances the proliferation of glioblastoma stem cells mainly by activating the transcription of mucin13 (MUC13). *Pharmazie*. 2017;72(2):98-102.

159. Sirito M, Lin Q, Deng JM, Behringer RR, Sawadogo M. Overlapping roles and asymmetrical cross-regulation of the USF proteins in mice. *Proc Natl Acad Sci U S A*. 1998;95(7):3758-3763.

160. Wood MA, Mukherjee P, Toocheck CA, Walker WH. Upstream stimulatory factor induces Nr5a1 and shbg gene expression during the onset of rat sertoli cell differentiation. *Biol Reprod*. 2011;85(5):965-976.

161. Viswanathan P, Wood MA, Walker WH. Follicle-stimulating hormone (FSH) transiently blocks FSH receptor transcription by increasing inhibitor of deoxyribonucleic acid binding/differentiation-2 and decreasing upstream stimulatory factor expression in rat sertoli cells. *Endocrinology*. 2009;150(8):3783-3791.

162. Burkhart DL, Sage J. Cellular mechanisms of tumour suppression by the retinoblastoma gene. *Nat Rev Cancer*. 2008;8(9):671-682.

163. Nevins JR. The rb/E2F pathway and cancer. *Hum Mol Genet*. 2001;10(7):699-703.

164. Ichimura K, Hanafusa H, Takimoto H, Ohgama Y, Akagi T, Shimizu K. Structure of the human retinoblastoma-related p107 gene and its intragenic deletion in a B-cell lymphoma cell line. *Gene*. 2000;251(1):37-43.

165. Wirt SE, Sage J. p107 in the public eye: An rb understudy and more. *Cell Div*. 2010;5:9-1028-5-9.

166. Classon M, Dyson N. P107 and P130: Versatile proteins with interesting pockets. *Exp Cell Res*. 2001;264(1):135-147.

167. Mulligan G, Jacks T. The retinoblastoma gene family: Cousins with overlapping interests. *Trends Genet*. 1998;14(6):223-229.

168. Lipinski MM, Jacks T. The retinoblastoma gene family in differentiation and development. *Oncogene*. 1999;18(55):7873-7882.

169. Hickman ES, Moroni MC, Helin K. The role of p53 and pRB in apoptosis and cancer. *Curr Opin Genet Dev*. 2002;12(1):60-66.

170. Bosco G, Du W, Orr-Weaver TL. DNA replication control through interaction of E2F-RB and the origin recognition complex. *Nat Cell Biol*. 2001;3(3):289-295.

171. Giacinti C, Giordano A. RB and cell cycle progression. *Oncogene*. 2006;25(38):5220-5227.

172. Iaquinta PJ, Lees JA. Life and death decisions by the E2F transcription factors. *Curr Opin Cell Biol*. 2007;19(6):649-657.

173. Moroni MC, Hickman ES, Lazzerini Denchi E, et al. Apaf-1 is a transcriptional target for E2F and p53. *Nat Cell Biol*. 2001;3(6):552-558.

174. Vigo E, Muller H, Prosperini E, et al. CDC25A phosphatase is a target of E2F and is required for efficient E2F-induced S phase. *Mol Cell Biol*. 1999;19(9):6379-6395.

175. Trimarchi JM, Lees JA. Sibling rivalry in the E2F family. *Nat Rev Mol Cell Biol*. 2002;3(1):11-20.

176. Di Stefano L, Jensen MR, Helin K. E2F7, a novel E2F featuring DP-independent repression of a subset of E2F-regulated genes. *EMBO J*. 2003;22(23):6289-6298.

177. Shan B, Durfee T, Lee WH. Disruption of RB/E2F-1 interaction by single point mutations in E2F-1 enhances S-phase entry and apoptosis. *Proc Natl Acad Sci U S A*. 1996;93(2):679-684.

178. Laresgoiti U, Apraiz A, Olea M, et al. E2F2 and CREB cooperatively regulate transcriptional activity of cell cycle genes. *Nucleic Acids Res*. 2013;41(22):10185-10198.

179. Liao Y, Du W. Rb-independent E2F3 promotes cell proliferation and alters expression of genes involved in metabolism and inflammation. *FEBS Open Bio*. 2017;7(10):1611-1621.

180. Gaubatz S, Lindeman GJ, Ishida S, et al. E2F4 and E2F5 play an essential role in pocket protein-mediated G1 control. *Mol Cell*. 2000;6(3):729-735.

181. Popov B, Chang LS, Serikov V. Cell cycle-related transformation of the E2F4-p130 repressor complex. *Biochem Biophys Res Commun*. 2005;336(3):762-769.

182. Yan W, Kero J, Suominen J, Toppari J. Differential expression and regulation of the retinoblastoma family of proteins during testicular development and spermatogenesis: Roles in the control of germ cell proliferation, differentiation and apoptosis. *Oncogene*. 2001;20(11):1343-1356.

183. El-Darwish KS, Parvinen M, Toppari J. Differential expression of members of the E2F family of transcription factors in rodent testes. *Reprod Biol Endocrinol*. 2006;4:63-7827-4-63.

184. Spiller CM, Wilhelm D, Koopman P. Retinoblastoma 1 protein modulates XY germ cell entry into G1/G0 arrest during fetal development in mice. *Biol Reprod*. 2010;82(2):433-443.

185. Hu YC, de Rooij DG, Page DC. Tumor suppressor gene rb is required for self-renewal of spermatogonial stem cells in mice. *Proc Natl Acad Sci U S A*. 2013;110(31):12685-12690.

186. Nalam RL, Andreu-Vieyra C, Braun RE, Akiyama H, Matzuk MM. Retinoblastoma protein plays multiple essential roles in the terminal differentiation of sertoli cells. *Mol Endocrinol*. 2009;23(11):1900-1913.

187. Field SJ, Tsai FY, Kuo F, et al. E2F-1 functions in mice to promote apoptosis and suppress proliferation. *Cell*. 1996;85(4):549-561.

188. Rotgers E, Nurmio M, Pietilä E, Cisneros-Montalvo S, Toppari J. E2F1 controls germ cell apoptosis during the first wave of spermatogenesis. *Andrology*. 2015;3(5):1000-1014.

189. Humbert PO, Rogers C, Ganiatsas S, et al. E2F4 is essential for normal erythrocyte maturation and neonatal viability. *Mol Cell*. 2000;6.

190. Danielian PS, Hess RA, Lees JA. E2f4 and E2f5 are essential for the development of the male reproductive system. *Cell Cycle*. 2016;15(2):250-260.

191. Kehoe SM, Oka M, Hankowski KE, et al. A conserved E2F6-binding element in murine meiosis-specific gene promoters. *Biol Reprod*. 2008;79(5):921-930.

192. Stan RV, Tkachenko E, Niesman IR. PV1 is a key structural component for the formation of the stomatal and fenestral diaphragms. *Mol Biol Cell*. 2004;15(8):3615-3630.

193. Stan RV. Structure of caveolae. *Biochim Biophys Acta*. 2005;1746(3):334-348.

194. Herrnberger L, Seitz R, Kuespert S, Bosl MR, Fuchshofer R, Tamm ER. Lack of endothelial diaphragms in fenestrae and caveolae of mutant plvap-deficient mice. *Histochem Cell Biol*. 2012;138(5):709-724.

195. Rantakari P, Auvinen K, Jäppinen N, et al. The endothelial protein PLVAP in lymphatics controls the entry of lymphocytes and antigens into lymph nodes. *Nat Immunol*. 2015;16(4):386-396.

196. Madden SL, Cook BP, Nacht M, et al. Vascular gene expression in nonneoplastic and malignant brain. *Am J Pathol*. 2004;165(2):601-608.

197. Tichauer KM, Deharvengt SJ, Samkoe KS, et al. Tumor endothelial marker imaging in melanomas using dual-tracer fluorescence molecular imaging. *Mol Imaging Biol*. 2014;16(3):372-382.

198. Strickland LA, Jubb AM, Hongo JA, et al. Plasmalemmal vesicle-associated protein (PLVAP) is expressed by tumour endothelium and is upregulated by vascular endothelial growth factor-A (VEGF). *J Pathol*. 2005;206(4):466-475.

199. Liu Y, Carson-Walter EB, Cooper A, Winans BN, Johnson MD, Walter KA. Vascular gene expression patterns are conserved in primary and metastatic brain tumors. *J Neurooncol*. 2010;99(1):13-24.

200. Wang YH, Cheng TY, Chen TY, Chang KM, Chuang VP, Kao KJ. Plasmalemmal vesicle associated protein (PLVAP) as a therapeutic target for treatment of hepatocellular carcinoma. *BMC Cancer*. 2014;14:815-2407-14-815.

201. Deharvengt SJ, Tse D, Sideleva O, et al. PV1 down-regulation via shRNA inhibits the growth of pancreatic adenocarcinoma xenografts. *J Cell Mol Med*. 2012;16(11):2690-2700.

202. Carson-Walter EB, Hampton J, Shue E, et al. Plasmalemmal vesicle associated protein-1 is a novel marker implicated in brain tumor angiogenesis. *Clin Cancer Res*. 2005;11(21):7643-7650.

203. Mozer AB, Whittemore SR, Benton RL. Spinal microvascular expression of PV-1 is associated with inflammation, perivascular astrocyte loss, and diminished EC glucose transport potential in acute SCI. *Curr Neurovasc Res*. 2010;7(3):238-250.

204. Hnasko R, McFarland M, Ben-Jonathan N. Distribution and characterization of plasmalemma vesicle protein-1 in rat endocrine glands. *J Endocrinol*. 2002;175(3):649-661.

205. Lecureuil C, Fontaine I, Crepieux P, Guillou F. Sertoli and granulosa cell-specific cre recombinase activity in transgenic mice. *Genesis*. 2002;33(3):114-118.

206. Marino S, Vooijs M, van Der Gulden H, Jonkers J, Berns A. Induction of medulloblastomas in p53-null mutant mice by somatic inactivation of rb in the external granular layer cells of the cerebellum. *Genes Dev*. 2000;14(8):994-1004.

207. Wu L, Timmers C, Maiti B, et al. The E2F1-3 transcription factors are essential for cellular proliferation. *Nature*. 2001;414(6862):457-462.

208. Asp P, Acosta-Alvear D, Tsikitis M, van Oevelen C, Dynlacht BD. E2f3b plays an essential role in myogenic differentiation through isoform-specific gene regulation. *Genes Dev*. 2009;23(1):37-53.

209. Cao AR, Rabinovich R, Xu M, Xu X, Jin VX, Farnham PJ. Genome-wide analysis of transcription factor E2F1 mutant proteins reveals that N- and C-terminal protein interaction domains do not participate in targeting E2F1 to the human genome. *J Biol Chem*. 2011;286(14):11985-11996.

210. van Casteren JI, Schoonen WG, Kloosterboer HJ. Development of time-resolved immunofluorometric assays for rat follicle-stimulating hormone and luteinizing hormone and application on sera of cycling rats. *Biol Reprod*. 2000;62(4):886-894.

211. Clermont Y, Perey B. Quantitative study of the cell population of the seminiferous tubules in immature rats. *Am J Anat*. 1957;100(2):241-267.

212. Wing TY, Christensen aK. Morphometric studies on rat seminiferous tubules. *Am J Anat*. 1982;165(1):13-25.

213. Rijntjes E, Swarts HJ, Anand-Ivell R, Teerds KJ. Prenatal induced chronic dietary hypothyroidism delays but does not block adult-type leydig cell development. *Am J Physiol Endocrinol Metab*. 2009;296(2):E305-14.

214. Hamer G, Roepers-Gajadien HL, van Duyn-Goedhart A, et al. DNA double-strand breaks and gamma-H2AX signaling in the testis. *Biol Reprod*. 2003;68(2):628-634.

215. Meyer-Ficca ML, Meyer RG, Jacobson EL, Jacobson MK. Poly(ADP-ribose) polymerases: Managing genome stability. *Int J Biochem Cell Biol*. 2005;37(5):920-926.

216. Roosen-Runge EC, Leik J. Gonocyte degeneration in the postnatal male rat. *Am J Anat*. 1968;122(2):275-299.

217. Reda A, Albalushi H, Montalvo SC, et al. Knock-out serum replacement and melatonin effects on germ cell differentiation in murine testicular explant cultures. *Ann Biomed Eng*. 2017;45(7):1783-1794.

218. Eggert A, Cisneros-Montalvo S, Anandan S, et al. The effects of perfluorooctanoic acid (PFOA) on fetal and adult rat testis. *Reprod Toxicol*. 2019;90:68-76.

219. Chen C, Ouyang W, Grigura V, et al. ERM is required for transcriptional control of the spermatogonial stem cell niche. *Nature*. 2005;436(7053):1030-1034.

220. Tokue M, Ikami K, Mizuno S, et al. SHISA6 confers resistance to differentiation-promoting wnt/beta-catenin signaling in mouse spermatogenic stem cells. *Stem Cell Reports*. 2017;8(3):561-575.

221. Ventela S, Mäkelä JA, Kulmala J, Westermarck J, Toppari J. Identification and regulation of a stage-specific stem cell niche enriched by nanog-positive spermatogonial stem cells in the mouse testis. *Stem Cells*. 2012;30(5):1008-1020.

222. Caires KC, de Avila J, McLean DJ. Endocrine regulation of spermatogonial stem cells in the seminiferous epithelium of adult mice. *Biores Open Access*. 2012;1(5):222-230.

223. Tadokoro Y, Yomogida K, Ohta H, Tohda A, Nishimune Y. Homeostatic regulation of germinal stem cell proliferation by the GDNF/FSH pathway. *Mech Dev*. 2002;113(1):29-39.

224. Sirito M, Walker S, Lin Q, Kozlowski MT, Klein WH, Sawadogo M. Members of the USF family of helix-loop-helix proteins bind DNA as homo- as well as heterodimers. *Gene Expr*. 1992;2(3):231-240.

225. Zimmermann C, Stevant I, Borel C, et al. Research resource: The dynamic transcriptional profile of sertoli cells during the progression of spermatogenesis. *Mol Endocrinol*. 2015;29(4):627-642.

226. Kong LJ, Chang JT, Bild AH, Nevins JR. Compensation and specificity of function within the E2F family. *Oncogene*. 2007;26(3):321-327.

227. Greenspan LJ, Matunis EL. Retinoblastoma intrinsically regulates niche cell quiescence, identity, and niche number in the adult drosophila testis. *Cell Rep*. 2018;24(13):3466-3476.e8.

228. Ziebold U, Reza T, Caron A, Lees JA. E2F3 contributes both to the inappropriate proliferation and to the apoptosis arising in rb mutant embryos. *Genes Dev*. 2001;15(4):386-391.

229. Ziebold U, Lee EY, Bronson RT, Lees JA. E2F3 loss has opposing effects on different pRB-deficient tumors, resulting in suppression of pituitary tumors but metastasis of medullary thyroid carcinomas. *Mol Cell Biol*. 2003;23(18):6542-6552.

230. Guo Q, Kumar TR, Woodruff T, Hadsell LA, DeMayo FJ, Matzuk MM. Overexpression of mouse follistatin causes reproductive defects in transgenic mice. *Mol Endocrinol*. 1998;12(1):96-106.

231. Archambeault DR, Yao HH. Loss of smad4 in sertoli and leydig cells leads to testicular dysgenesis and hemorrhagic tumor formation in mice. *Biol Reprod*. 2014;90(3):62.

232. Ahmed EA, Barten-van Rijbroek AD, Kal HB, et al. Proliferative activity in vitro and DNA repair indicate that adult mouse and human sertoli cells are not terminally differentiated, quiescent cells. *Biol Reprod*. 2009;80(6):1084-1091.

233. Hamer G, Roepers-Gajadien HL, van Duyn-Goedhart A, et al. Function of DNA-protein kinase catalytic subunit during the early meiotic prophase without Ku70 and Ku86. *Biol Reprod*. 2003;68(3):717-721.

234. Hamer G, Kal HB, Westphal CH, Ashley T, de Rooij DG. Ataxia telangiectasia mutated expression and activation in the testis. *Biol Reprod*. 2004;70(4):1206-1212.

235. Beumer TL, Roepers-Gajadien HL, Gademan IS, et al. The role of the tumor suppressor p53 in spermatogenesis. *Cell Death Differ*. 1998;5(8):669-677.

236. Zheng N, Fraenkel E, Pabo CO, Pavletich NP. Structural basis of DNA recognition by the heterodimeric cell cycle transcription factor E2F-DP. *Genes Dev*. 1999;13(6):666-674.

237. Keuschnigg J, Henttinen T, Auvinen K, Karikoski M, Salmi M, Jalkanen S. The prototype endothelial marker PAL-E is a leukocyte trafficking molecule. *Blood*. 2009;114(2):478-484.

238. Minshall RD, Malik AB. Transport across the endothelium: Regulation of endothelial permeability. *Handb Exp Pharmacol*. 2006;(176 Pt 1):107-44. doi(176 Pt 1):107-144.

239. Abel MH, Wootton AN, Wilkins V, Huhtaniemi I, Knight PG, Charlton HM. The effect of a null mutation in the follicle-stimulating hormone receptor gene on mouse reproduction. *Endocrinology*. 2000;141(5):1795-1803.

240. Kumar TR, Wang Y, Lu N, Matzuk MM. Follicle stimulating hormone is required for ovarian follicle maturation but not male fertility. *Nat Genet*. 1997;15(2):201-204.

241. Nes WD, Lukyanenko YO, Jia ZH, et al. Identification of the lipophilic factor produced by macrophages that stimulates steroidogenesis. *Endocrinology*. 2000;141(3):953-958.

242. Lukyanenko YO, Chen JJ, Hutson JC. Production of 25-hydroxycholesterol by testicular macrophages and its effects on leydig cells. *Biol Reprod*. 2001;64(3):790-796.

243. Claudio PP, Howard CM, Fu Y, et al. Mutations in the retinoblastoma-related gene RB2/p130 in primary nasopharyngeal carcinoma. *Cancer Res*. 2000;60(1):8-12.

244. Helin K, Holm K, Niebuhr A, et al. Loss of the retinoblastoma protein-related p130 protein in small cell lung carcinoma. *Proc Natl Acad Sci USA*. 1997;94(13):6933-6938. doi: 10.1073/pnas.94.13.6933.

245. Murga M, Fernandez-Capetillo O, Field SJ, et al. Mutation of E2F2 in mice causes enhanced T lymphocyte proliferation, leading to the development of autoimmunity. *Immunity*. 2001;15.

246. Sanchez AP, Zhao J, You Y, Decleves AE, Diamond-Stanic M, Sharma K. Role of the USF1 transcription factor in diabetic kidney disease. *Am J Physiol Renal Physiol*. 2011;301(2):F271-9.

247. Hermann BP, Hornbaker K, Rice DA, Sawadogo M, Heckert LL. In vivo regulation of follicle-stimulating hormone receptor by the transcription factors upstream stimulatory factor 1 and upstream stimulatory factor 2 is cell specific. *Endocrinology*. 2008;149(10):5297-5306.

248. Toocheck C, Clister T, Shupe J, et al. Mouse spermatogenesis requires classical and nonclassical testosterone signaling. *Biol Reprod*. 2016;94(1):11.

249. Zhang FP, Pakarainen T, Poutanen M, Toppari J, Huhtaniemi I. The low gonadotropin-independent constitutive production of testicular testosterone is sufficient to maintain spermatogenesis. *Proc Natl Acad Sci U S A*. 2003;100(23):13692-13697.

250. Jäppinen N, Felix I, Lokka E, et al. Fetal-derived macrophages dominate in adult mammary glands. *Nat Commun*. 2019;10(1):281-018-08065-1.

UNIVERSITY OF TURKU